FIRST H.F. DOPPLER SOUNDINGS OF THE IONOSPHERE AT SANAE

by

Errol James de Kock

A thesis submitted in fulfilment of the requirements for the degree of Master of Science of Rhodes University.

December, 1979.

CONTENTS

CHAPTER 1

INTRODUCTION

Since 1962 the Rhodes Antarctic Research Group has operated an ionosonde at the South African Antarctic base SANAE. Initial soundings were made by means of a pulse ionosonde, but in 1975 a chirp ionosonde (described in Chapter 2) was installed and is capable of both vertical and oblique soundings. A similar ionosonde has been in operation in Grahamstown from 1973.

Research has centred on the anomalies (the South Atlantic Anomaly and the Southern Anomaly) over the Southern Ocean as well as on disturbances or movements in the ionosphere, for example, Travelling Ionospheric Disturbances, movements of the mid-latitude trough and particle precipitation.

A very powerful tool for detecting movements in the ionosphere is the H.F. Doppler technique, developed and described by Watts and Davies (1960). A number of groups have used the technique and have reported interesting results, often associated with geophysical phenomena (e.g. Cornelius et al (1975), Dudeney et al (1977), Chan et al (1962a,b) and Huang et al (1973)). Stations using this technique cover a wide range of latitudes and both vertical and oblique paths have been used in the observations.

During 1977 Mr. Allon Poole of our Research Group showed that it was relatively easy to convert the Chirpsounder into a vertical Doppler sounder and thus it is possible to use this

equipment to detect movements in the ionosphere. The technique was initially tested on the ionosonde in Grahamstown and during 1978 similar modifications were made by the author to the Chipsounder in operation at SANAE.

A number of observations were made at SANAE during 1978 and are continuing at present. Both magnetically disturbed as well as quiet periods were used for the observations which have proved to be very interesting. The observations made, using the Chirpsounder, differ from most others in that a relatively long integration time is used on the spectrum analyser, resulting in better frequency resolution after Fourier transformation. Initial impressions of the data can be misleading as a result of the long integration time and overlapping window analysis, but an understanding of the theory involved shows how interpretation of the data is to be approached.

This thesis describes the results of the preliminary study undertaken during 1978 and some initial interpretations of the data will be made. Suggestions for further work in this interesting field are made at various stages as well as suggestions regarding the improvement of the technique as it applies to the Chirpsounder.

Chapter 2 contains the principles of operation of the Chirpsounder and a description of its use as a Doppler Sounder. Data recorded during 1978 are shown in Chapter 3 together with the associated ionograms. Data recorded during 1979 have not

been analysed as they will only be available in South Africa after the relief voyage during January/February 1980. A description of the type of data expected and times of recording is given, however. Theory associated with Doppler sounding of the ionosphere is reviewed in Chapter 4.

Chapter 5 contains an analysis and suggestions as to the interpretation of the 1978 data while Chapter 6 contains some conclusions drawn from this initial study using the HF Doppler technique.

CHAPTER 2

OPERATION OF THE CHIRPSOUNDER AND DOPPLER MODE OPERATION

2.1 Chirpsounding Principles

In the chirp or FM CW ionosonde, as opposed to the pulse ionosonde, a synthesised frequency ramp (with the frequency increasing linearly with time) is transmitted. Provided that the sweep time is long compared to the signal travel time, the received signal is offset in frequency from the transmitted signal. This offset is proportional to the signal travel time, Δt, so that

$$\Delta f = k\Delta t \ , \qquad 2.1$$

where Δf is the offset frequency,

and $k = \frac{df}{dt}$, the linear sweep rate. 2.2

The normal use of an ionosonde is the measurement of the virtual height, h', of the reflection point as a function of frequency, f, defined by

$$h'(f) = \tfrac{1}{2} c \, \Delta t(f) \ , \qquad 2.3$$

where c is the speed of light in vacuo,

and Δt is the signal travel time.

A pulse ionosonde measures Δt directly whereas the Chirpsounder measures Δf which is proportional to Δt as given by equation 2.1.

If the received frequency is mixed with a sweeping local oscillator frequency and suitably filtered, a beat frequency equal to Δf is produced which can be resolved by a spectrum analyser. The analysis range of the spectrum analyser is determined by the sweep rate and the desired delay time range.

The effective bandwidth is very small, allowing low transmitter power to be used, without degrading the signal to noise ratio. Isolation of the transmitter and receiver is achieved by gating the transmitter and receiver on alternately using a T/R gating technique.

A block diagram of the chirpsounder is shown in Figure 2.1 The stable quartz oscillator, programmable frequency synthesiser and variable range spectrum analyser make the basic chirpsounder suitable for use as a Doppler sounder. The easy measurement of Δf makes it possible to use the chirpsounder as a Doppler sounder, with very little modification.

2.2 Chirpsounder as a Doppler Sounder

Doppler sounding of the ionosphere requires a fixed frequency to be transmitted which may undergo a small shift in frequency, δf, during its passage through, or reflection from, the ionosphere (δf is typically of the order of a few Hz). In order to observe both positive and negative shifts, it is necessary

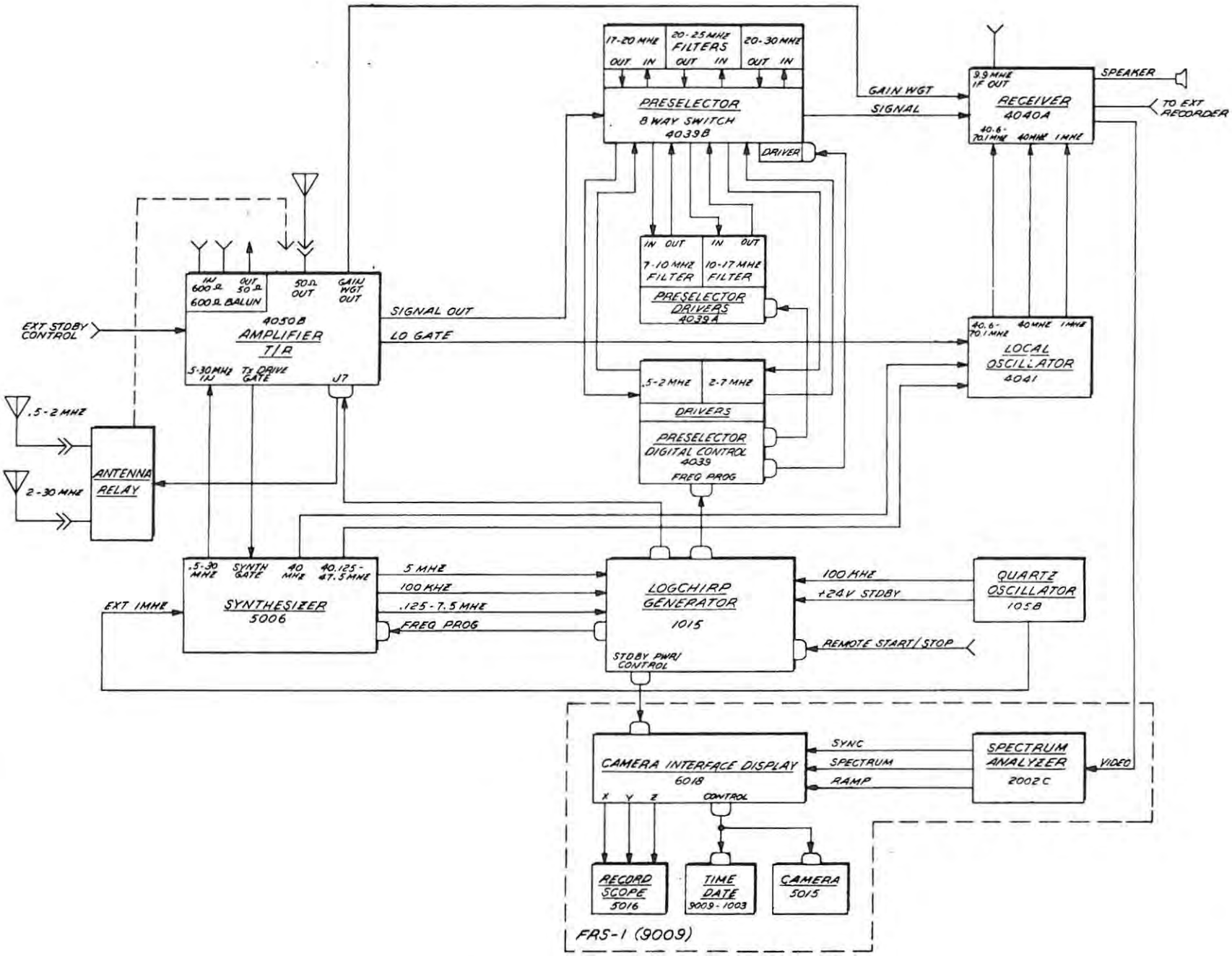

Figure 2.1 Vertichirp Sounder Block Diagram

to introduce an offset of a few Hz in the local oscillator frequency. Frequency stability in both the transmitted signal and the local oscillator signal, in addition to resolution of small frequency differences between the transmitted and received signals, is essential to any H.F. Doppler system. As mentioned before, the chirpsounder fulfils these basic requirements without any additional equipment or modification.

When using the chirpsounder as a Doppler sounder, use is made of some of the versatility of the equipment in its standard form. The transmitted signal is derived by amplifying an accurate and stable 5 MHz signal available from the quartz oscillator. During normal operation, this transmitted frequency is obtained from the synthesiser which is programmed to produce the required frequency by the Logchirp Control, the controlling unit of the chirpsounder. In addition to producing this signal, the synthesiser produces a signal which is used by the local oscillator unit to produce its local oscillator frequency, to be mixed with the received signal. The signal required by the local oscillator unit is of frequency

$$f_s = f_p + 40.0 \quad \text{(all in MHz)} \qquad 2.4$$

where f_p is the programmed frequency (as programmed by Logchirp Control) and is equal to quarter of the transmitted frequency (in normal operation),
and f_s is the synthesised frequency.

The local oscillator frequency, f_L, is related to this frequency, f_s, by

$$f_L = 4 f_s - 119.9 \quad \text{(all in MHz)} \quad 2.5$$

or using equation 2.4,

$$f_L = 4 f_p + 160.0 - 119.9 \text{ (all in MHz)}$$

$$= 4 f_p + 40.1 \quad \text{(all in MHz)} \quad 2.6$$

The received signal differs in frequency from the transmitted signal by an amount depending on the signal travel time (in normal operation) as given by equation 2.1. In Doppler mode however, the difference is dependent on movements of the reflecting layer or redistribution of ionization during the passage of the signal through the ionosphere, as the transmitted frequency is constant.

The offset required for Doppler mode operation is introduced by programming of the synthesiser from Logchirp control. The programmed frequency, f_p, in Doppler mode is given by

$$f_p = \tfrac{1}{4} (f_T + f_o) \quad , \quad 2.7$$

where f_T is the transmitted frequency,

and f_o is the offset frequency.

For all the Doppler work undertaken so far, f_T has been 5MHz and f_o set at 4Hz by means of a switch installed by the author for that purpose.

The 40.1 MHz intermediate frequency which is present after mixing the received signal with the local oscillator signal is removed in the receiver in two stages (mixing with 40 MHz, filtering and mixing with 100kHz, filtering). The signal which remains after this mixing is in a suitable form for spectrum analysis, to produce an ionogram (normal operation) or a Doppler record (Doppler mode). In order to prevent aliasing in the spectrum analyser, a low pass filter with cut off 10Hz is inserted in the signal path immediatly before the spectrum analyser for Doppler mode operation.

The usual frequency sweep which operates in normal mode is not used in Doppler mode for obvious reasons and must be disabled. All that is required is gating on of the transmitter and receiver alternately. For routine sounding this is under the control of logchirp control, but for Doppler mode, the T/R gating must be enabled by means of a multiposition switch (once again, the switch is available without alteration to the equipment). The basic T/R waveform used is shown in Figure 2.2 .

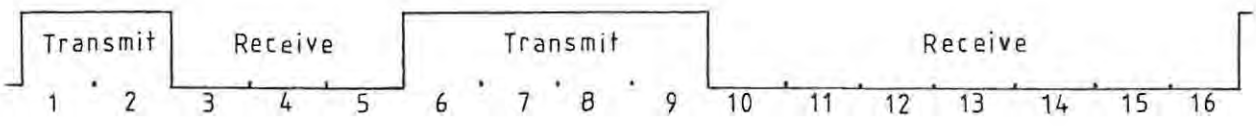

Figure 2.2

T/R Waveform

The sequence is made up of 16 segments, generated from a clock running at a minimum frequency of 5280Hz so that each segment is a maximum of 188 μsec long. This pattern is repeated throughout the sounding. A fixed repetition frequency results in a "blind range" and this effect is partially overcome by varying this repetition frequency. The clock frequency is "warbled" (frequency modulated) by a 1 Hz sawtooth waveform that causes the basic frequency to change between 5280 and 5808 Hz.

A switch was installed to allow the film recording system to be enabled independently of Logchirp control, completing the Doppler system of the chirpsounder.

Before proceeding to describe the Doppler experiment, mention must be made of the method of spectrum analysis employed in the chirpsounder as it differs from most standard methods. In order to perform any spectrum analysis on a real signal, the time series must be sampled at a frequency above the Nyquist rate and these samples are then spectrum analysed. This spectrum analysis can be carried out using a Fast Fourier Transform Algorithm or similar standard technique. The chirpsounder uses a frequency translation system combined with a filter.

The usual technique employed is to sample until the memory is full and then to transform the contents of the memory. This cycle is repeated so that a transform is obtained whenever sufficient samples have been taken to fill the memory. The system

used in the chirpsounder differs in that it updates the memory (1200 x 8-bit words) whenever there is a new sample present. A transform of the contents of the memory is obtained every 100μs. Updating is such that the oldest sample in memory is replaced each time there is a new sample. This "overlapping window" has the effect of smearing the transform. The sampling frequency used in the spectrum analyser is always three times the analysis range selected (Nyquist theorem requires that it be at least twice the maximum frequency component present). Some theory dealing with the spectrum analysis and its effect on the data is described in Chapter 4.

A block diagram of the chirpsounder as set up for the Doppler experiment (Transmitting at 5MHz and with 4Hz offset) is shown in Figure 2.3.

2.3 The Doppler Experiment

The Doppler experiment described here was initiated during 1978 in order to obtain data from a high-latitude station, using the chirpsounder as a Doppler sounder. All observations described were recorded at South Africa's Antarctic base, SANAE.

For the experiment, the Barry Research Vertichirp VOS-1C ionosonde of the Antarctic Research Group, Physics and Electronics

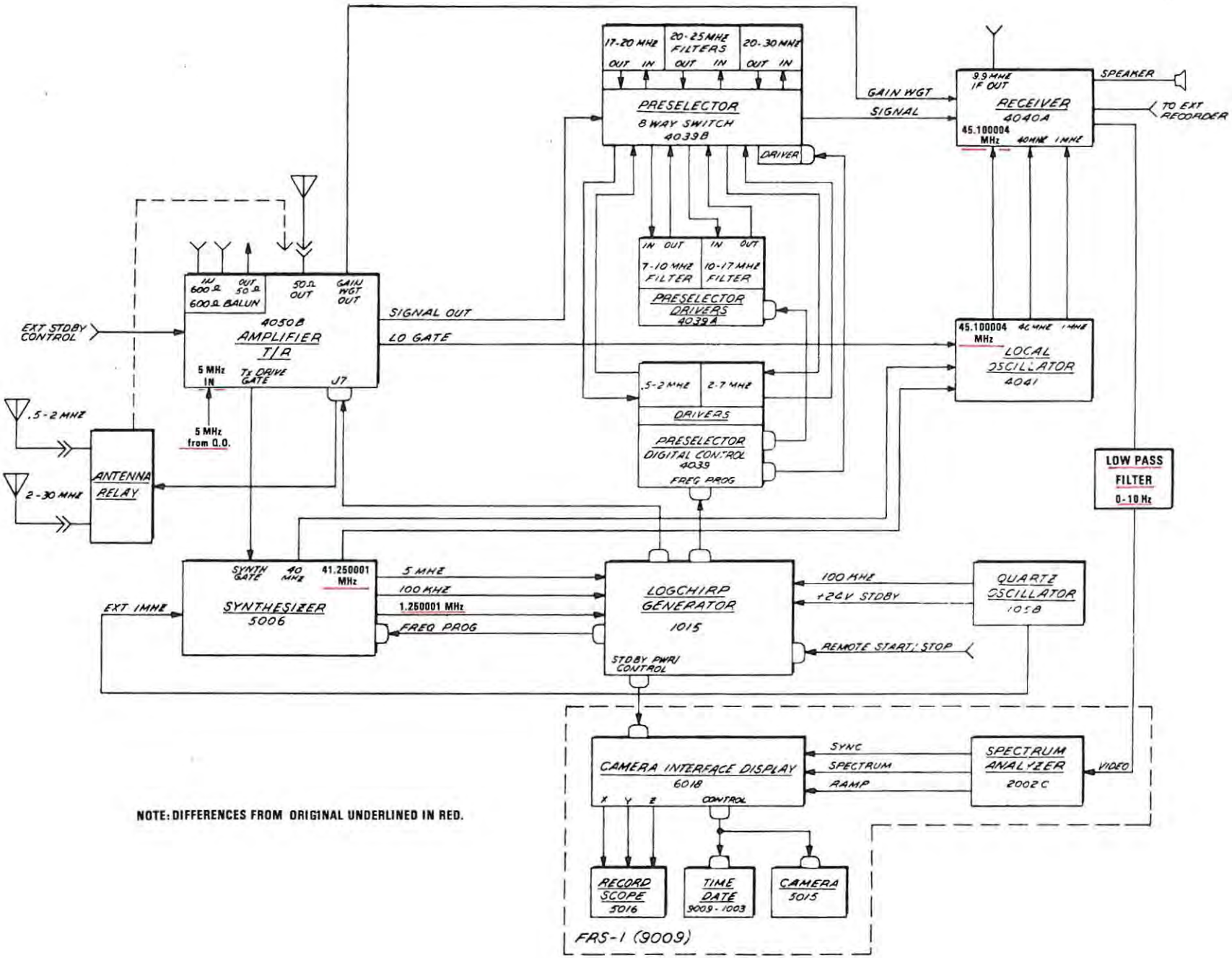

NOTE: DIFFERENCES FROM ORIGINAL UNDERLINED IN RED.

Figure 2.3 Chirpsounder in Doppler Mode Block Diagram
(5MHz with 4Hz offset)

Department, Rhodes University was used, set up in Doppler mode as described in section 2.2 and shown in Figure 2.3

Transmission and reception were by means of a single antenna, a vertical delta, with dimensions as shown in Figure 2.4.

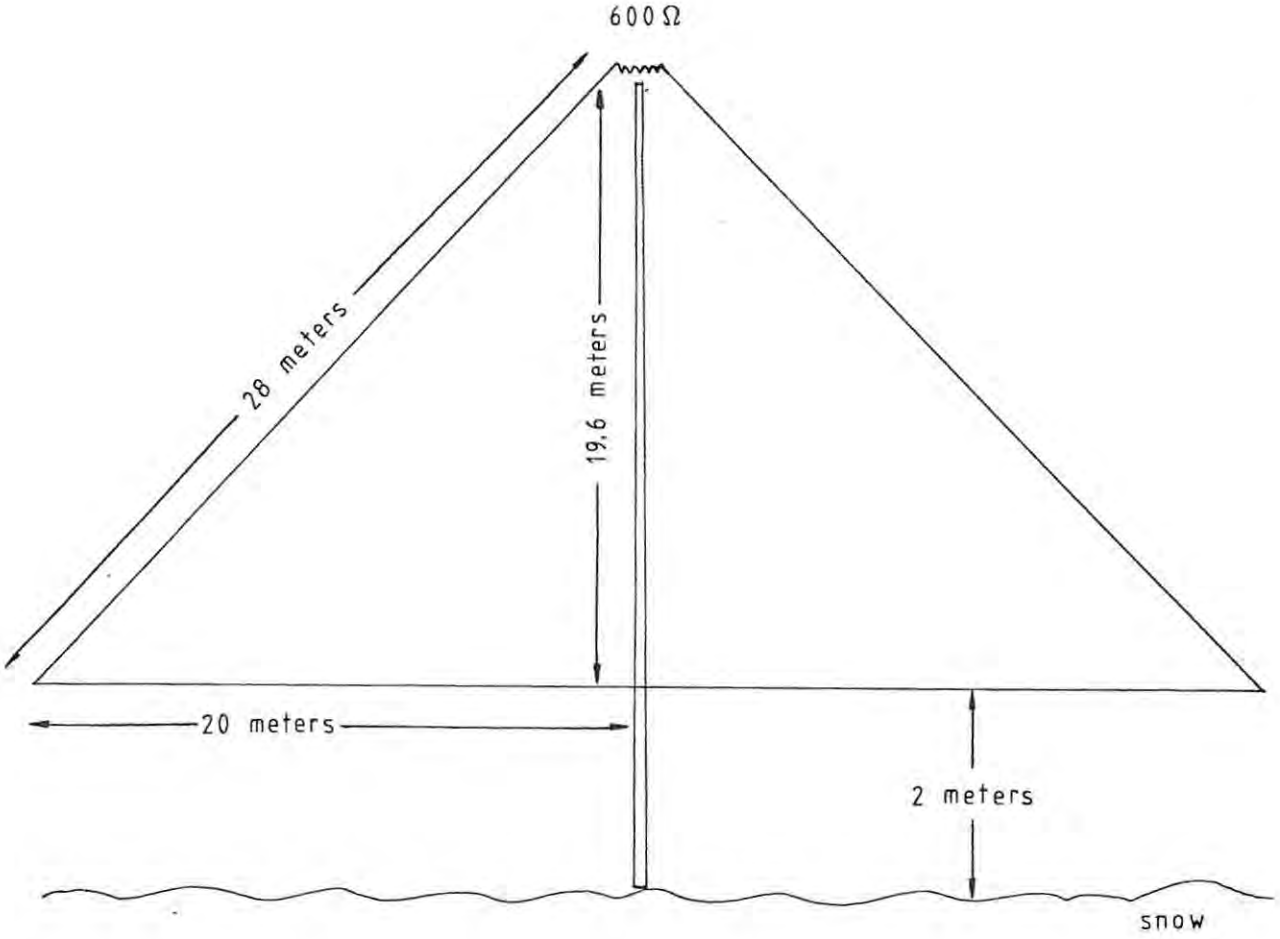

Figure 2.4

Dimensions of Delta Antenna

Transmitter output power is specified as 8 watts (peak, nominal) and 3 watts (average, nominal). As a frequency standard, the ionosonde uses a Hewlett Packard Quartz Oscillator 105B which is specified as having a maximum rms fractional frequency deviation

in the short term (due to random noise) of 10^{-11}(for 5MHz output). This corresponds to a maximum of 5 x 10^{-5}Hz variation from a frequency of 5MHz averaging for 20s and with at least 100 samples. The spectrum analyser was used with an analysis range of 0-10 Hz, and recording was made on photographic film in the same way as normal ionograms are recorded.

The following are details of the station SANAE :

Geographic latitute	:	70° 19' 12" S (-70.3200°)
Geographic longitude	:	2° 22' 20" W (-2.3722°)
Geomagnetic latitute	:	57.2° S
Geomagnetic longitude	:	34.7° E
Electron gyrofrequency	:	1.18 MHz
Magnetic dip angle	:	-62.50°
Magnetic declination	:	19.12°W
L value at 0 km	:	3.98

One of the major advantages of using SANAE for these investigations is that there are a number of routine recordings continuously being made that can provide additional information when analysing the Doppler records. A magnetometer, micropulsation system, riometers and a seismograph are in continuous operation in addition to routine meterological observations. Whistlers are recorded during active times and a number of auroral observations are made during the dark hours. Airglow photometers, an all-sky camera and a video auroral recording system provide these data. It is unfortunate that no

ionograms can be recorded during Doppler soundings but it is hoped that this may be possible in the near future when the control units of the chirpsounder will be replaced by a microprocessor and a number of additional facilities will be introduced. At present, Doppler recordings are kept reasonably short so that routine ionogram data are obtained with a minimum of loss.

For data observed during 1978, the first of a set of five recordings was chosen to start when a fairly intense magnetic storm was in progress. Recordings lasted, on average, 30 minutes per day for five successive days, at the same time each day. Three periods of five-day recordings were made, one each during winter, equinox and summer. During the first two periods, care had to be taken to ensure that 5MHz was not above the critical frequency of the F_2-layer during Doppler soundings. During summer, this was not as important, since f_oF_2 was above 5MHz for a large part of the day. Using this routine resulted in both magnetically quiet and disturbed recording periods.

Radio "blackout" was often a problem if the magnetic storm increased in intensity during the five-day recording period, usually resulting in a "blackout"of the Doppler data as well.

Most of the discussion (in Chapter 5) as well as the conclusions drawn (in Chapter 6) concern the 1978 data, the first results of this experiment.

CHAPTER 3

DOPPLER DATA AND ASSOCIATED IONOGRAMS

1978 SANAE Data

As mentioned earlier, recordings during 1978 were made during winter, equinox and summer, each period being for five consecutive days at the same time each day. Table 3.1 contains details concerning the times and dates of the recordings.

Table 3.1
Summary of 1978 SANAE Doppler Data

Date	Day No.	Time of recording	Comments
2/6/78	153	12:06 - 12:44 UT	
3/6/78	154	12:06 - 12:44 UT	
4/5/78	155	12:06 - 12:44 UT	
5/6/78	156	12:06 - 12:44 UT	"Blackout" - no record
6/6/78	157	12:06 - 12:44 UT	"Blackout" - no record
12/8/78	224	11:36 - 11:58 UT	"Blackout" - no record
13/8/78	225	11:36 - 11:58 UT	Absorption of frequencies to above 5MHz
14/8/78	226	11:36 - 11:58 UT	
15/8/78	227	11:36 - 11:58 UT	
16/8/78	228	11:36 - 11:58 UT	
12/12/78	346	19:10 - 19:45 UT	
13/12/78	347	19:10 - 19:45 UT	Instrumental problems - no record
14/12/78	348	19:10 - 19:45 UT	
15/12/78	349	19:10 - 19:45 UT	Partial blackout - only very slight signal
16/12/78	350	19:10 - 19:45 UT	"Blackout" - no record

As can be seen from the table above, ionospheric absorption of radio waves (causing either complete or partial blackout of the ionograms) was responsible for most of the loss of Doppler data during 1978. The nine remaining records are shown, together with the ionogram immediately before the recording and that immediately afterward, in Figures 3.1 through 3.9.

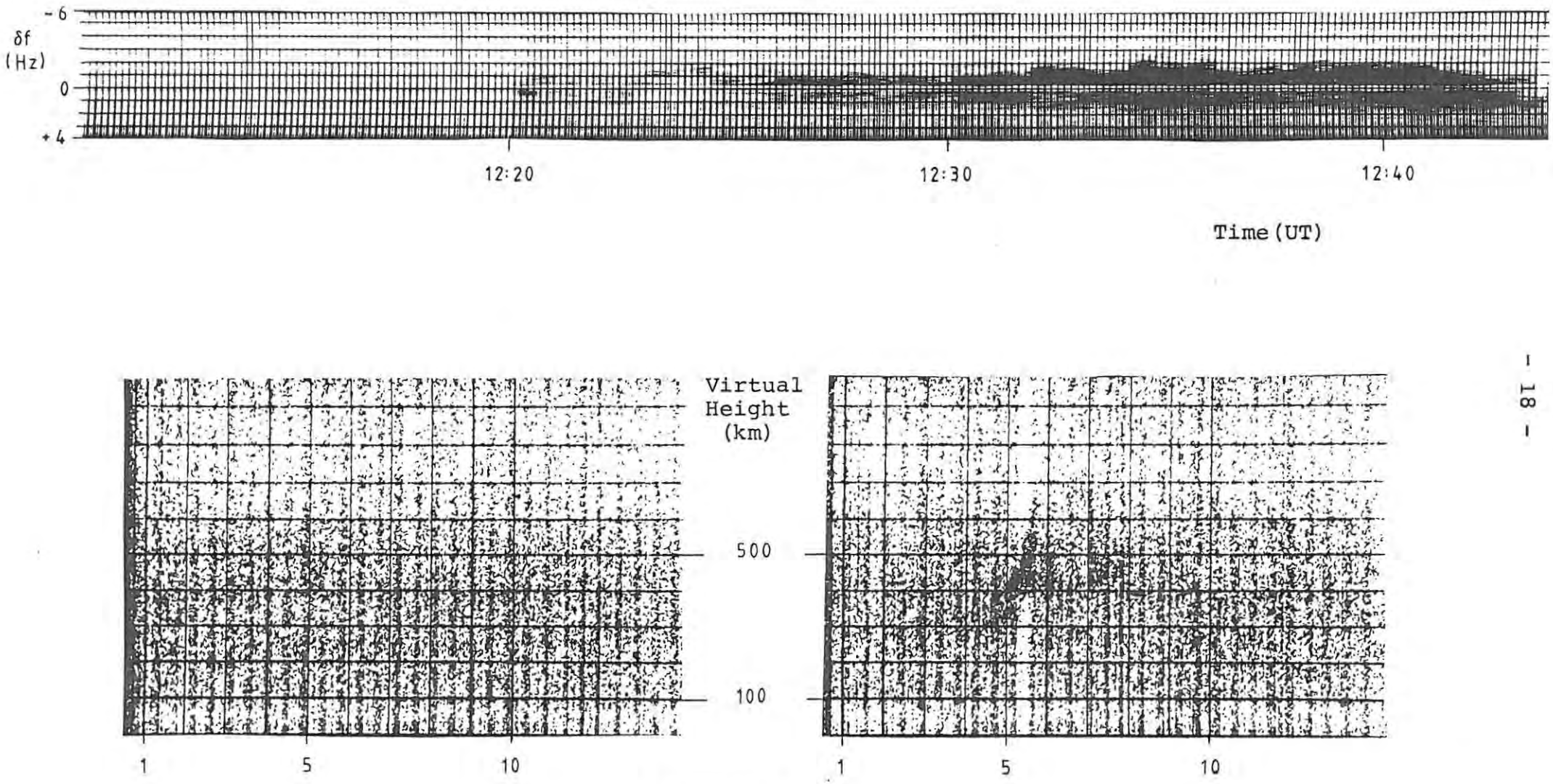
-6
δf
(Hz)
0
+4
12:20
12:30
12:40
Time (UT)
Virtual
Height
(km)
500
100
1
5
10
1
5
10
Frequency (MHz)
12:00UT
4th June, 1978 - day 153 - SANAE
12:45UT

Figure 3.1

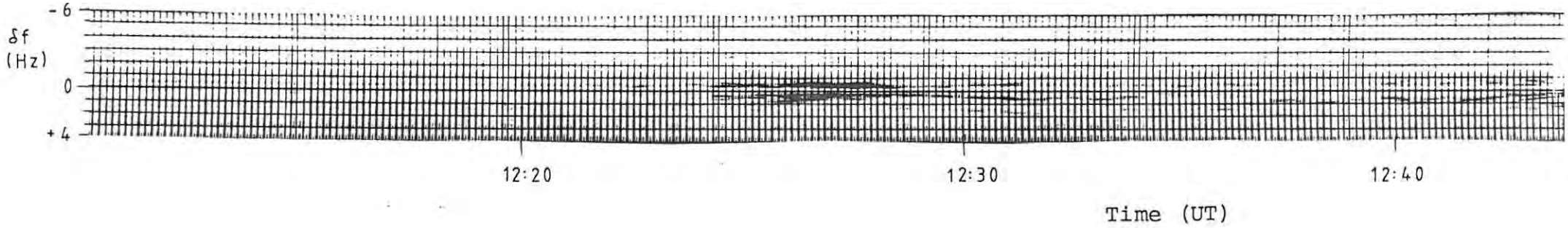

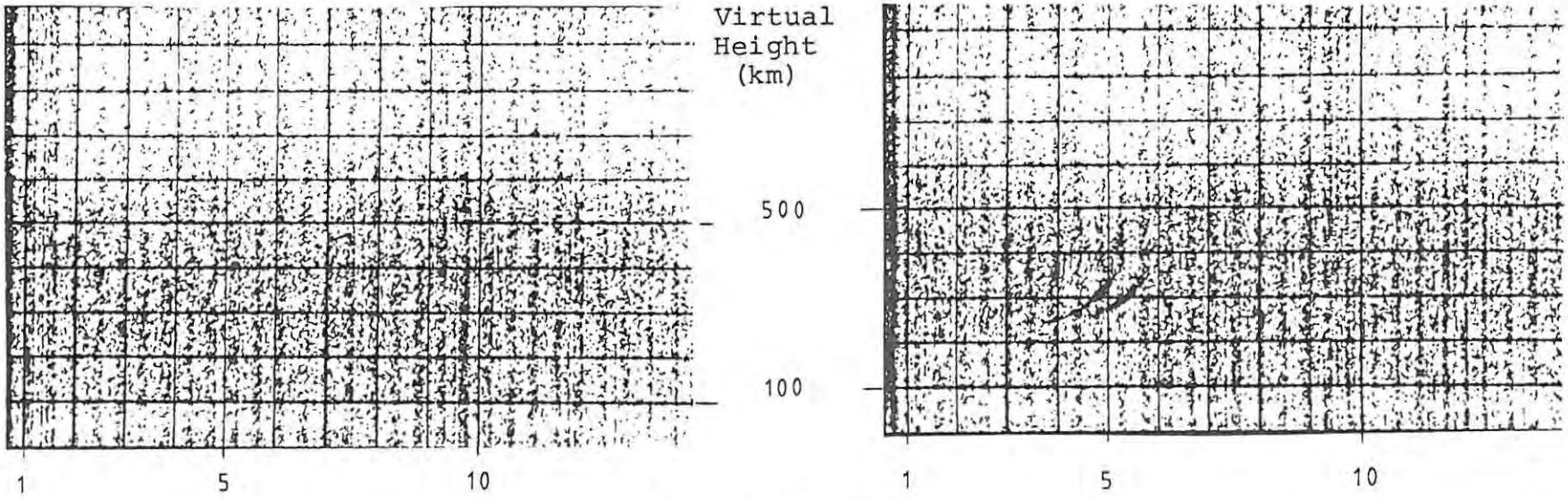

12:00UT 3rd June,1978 - day 154 - SANAE 12:45UT

Figure 3.2

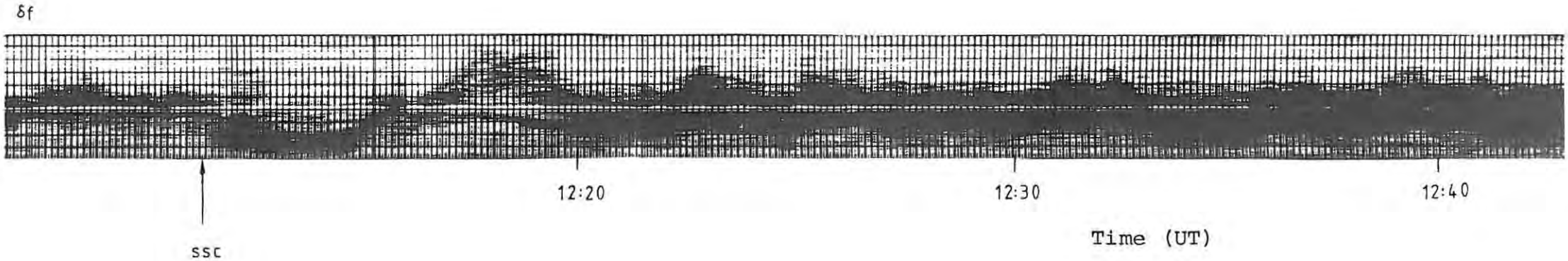
δf
12:20
12:30
12:40
ssc
Time (UT)

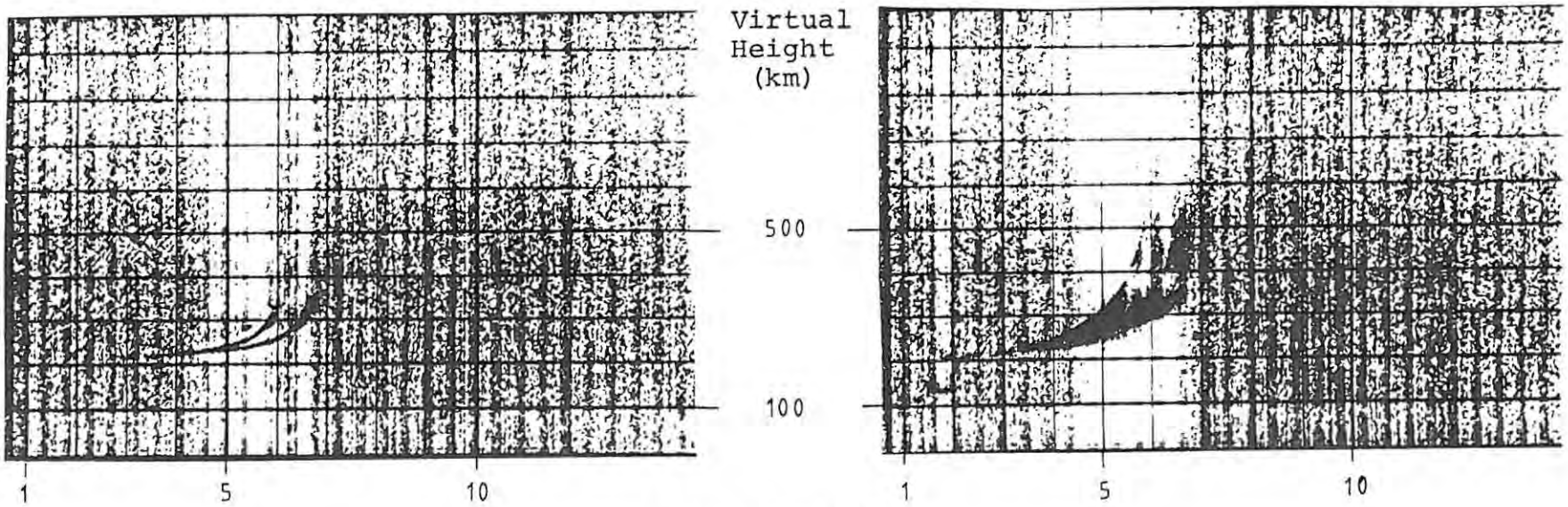
Virtual
Height
(km)
500
100
1
5
10
1
5
10
Frequency (MHz)
12:00UT
4th June,1978 - day 155 - SANAE
12:45UT

Figure 3.3

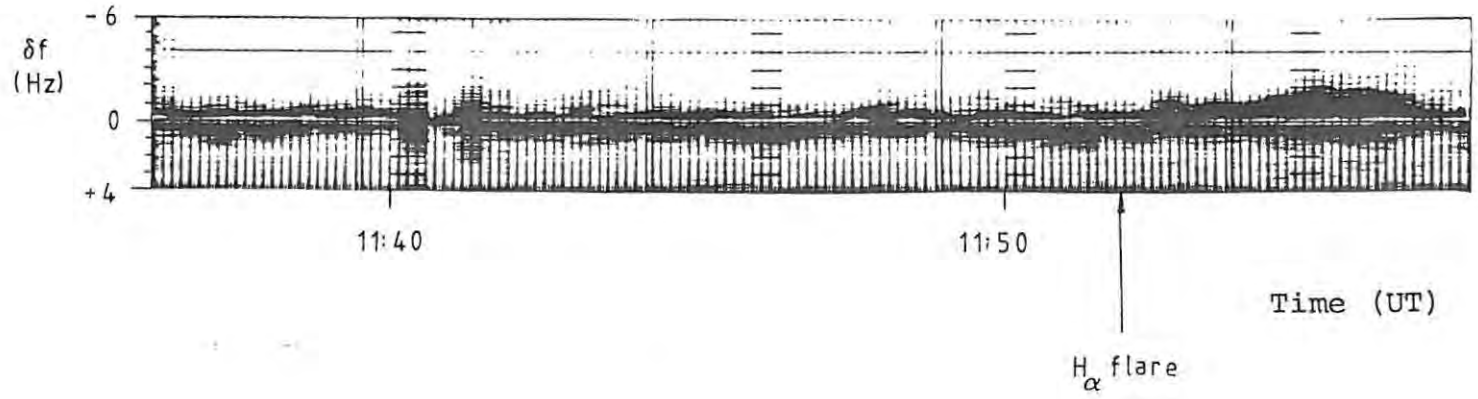
-6
δf
(Hz)
0
+4
11:40
11:50
Time (UT)
H_α flare

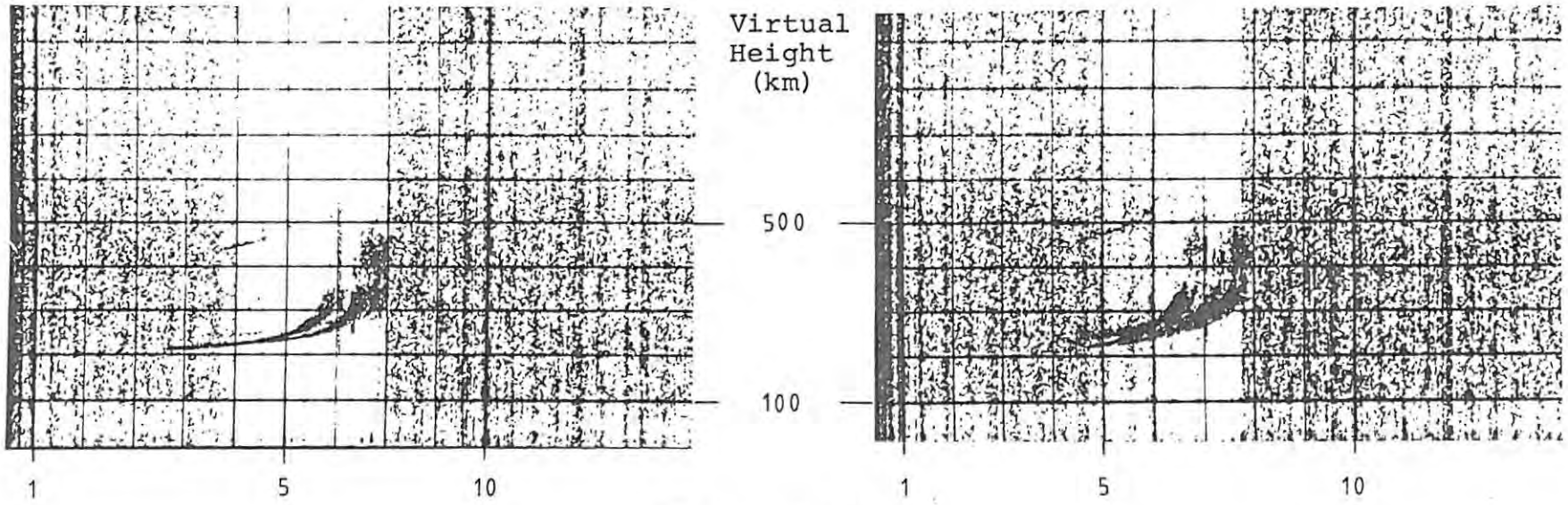
Virtual
Height
(km)
500
100
1
5
10
1
5
10
Frequency (MHz)
11:30UT
14th August,1978 - day 226 - SANAE
12:00UT

Figure 3.4

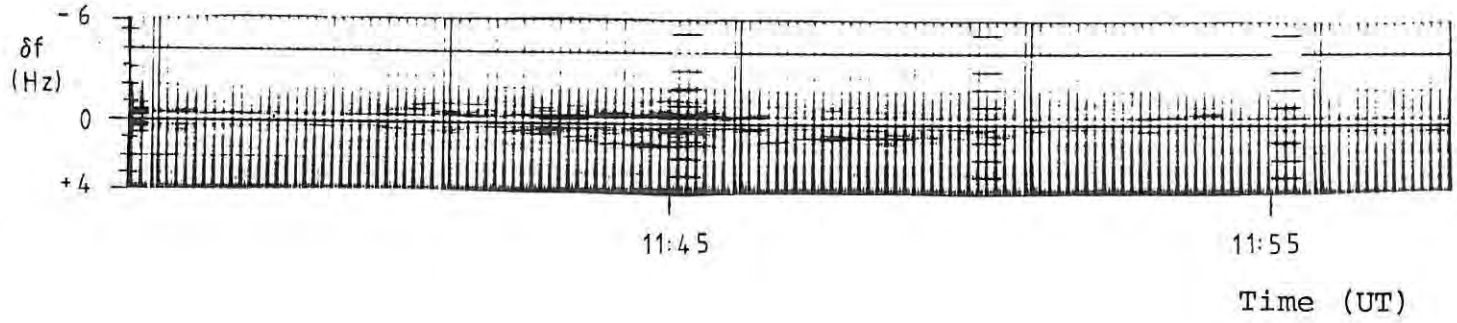
- 6
δf
(Hz)
0
+4
11:45
11:55
Time (UT)

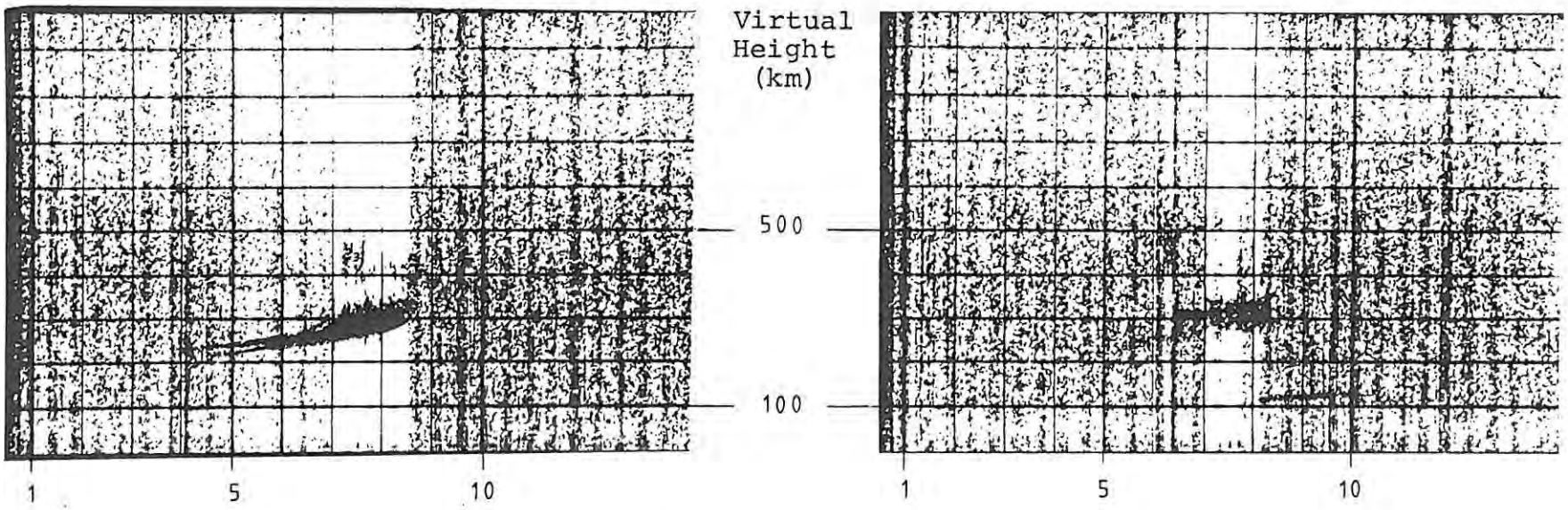
Virtual
Height
(km)
500
100
1
5
10
1
5
10
Frequency (MHz)
11:30UT
15th August,1978 - day 227 - SANAE
12:00UT

Figure 3.5

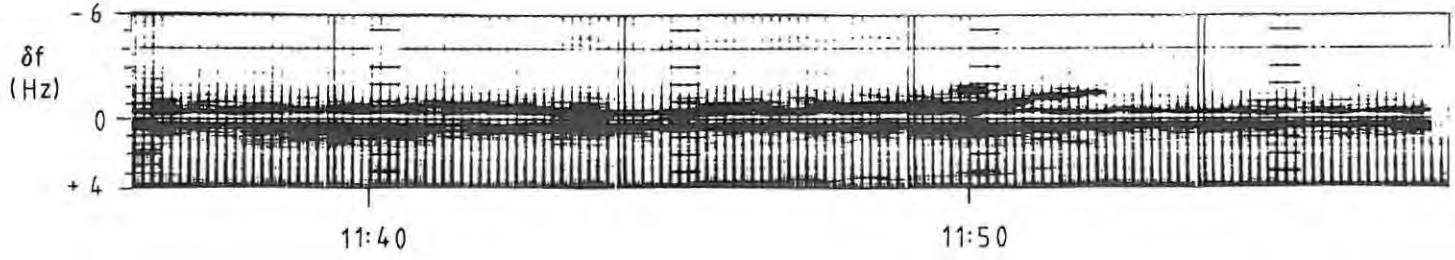
- 6
δf
(Hz)
0
+ 4
11:40
11:50
Time (UT)

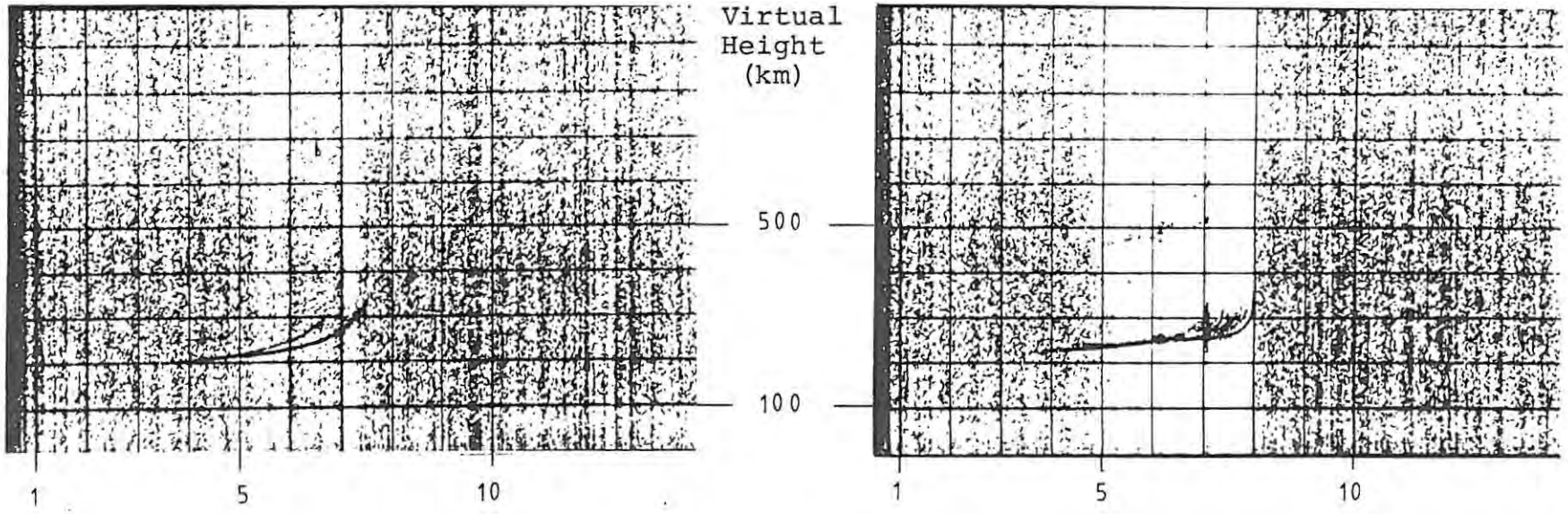
Virtual
Height
(km)
500
100
1
5
10
1
5
10
Frequency (MHz)
11:30UT
16th August,1978 - day 228 - SANAE
12:00UT

Figure 3.6

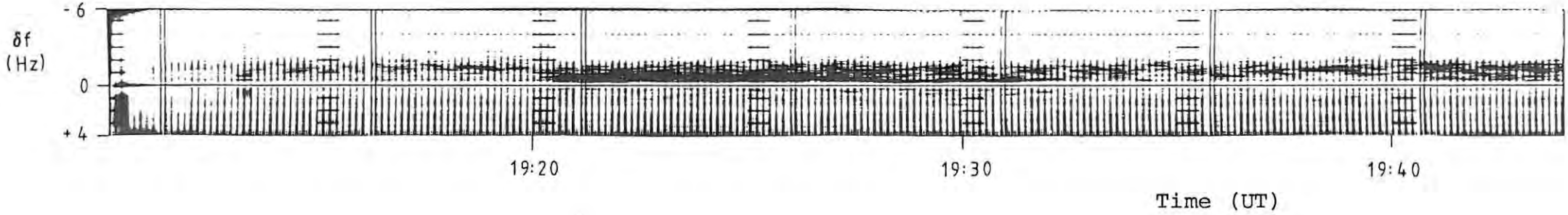

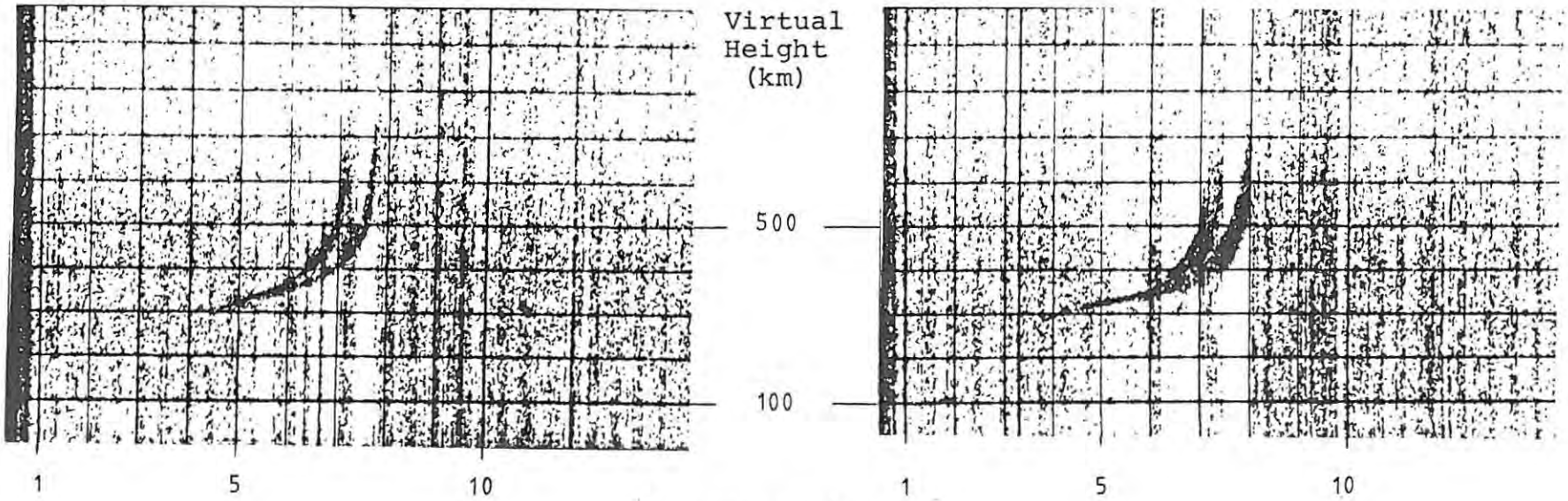

19:00UT 12th December,1978 - day 346 - SANAE 19:45UT

Figure 3.7

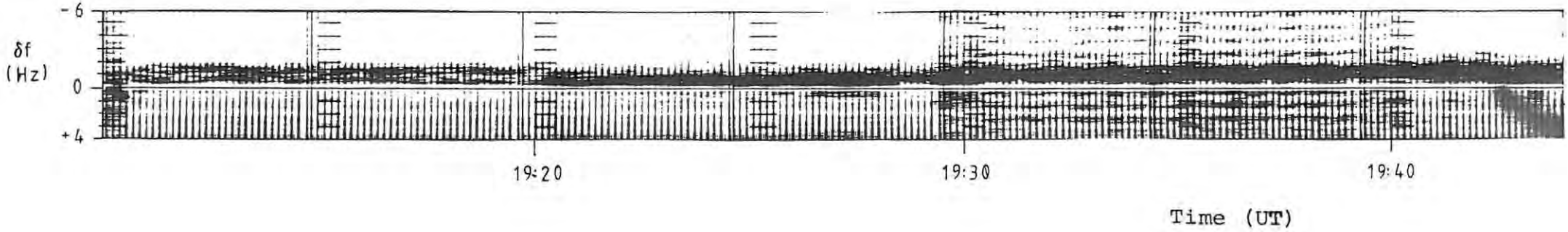

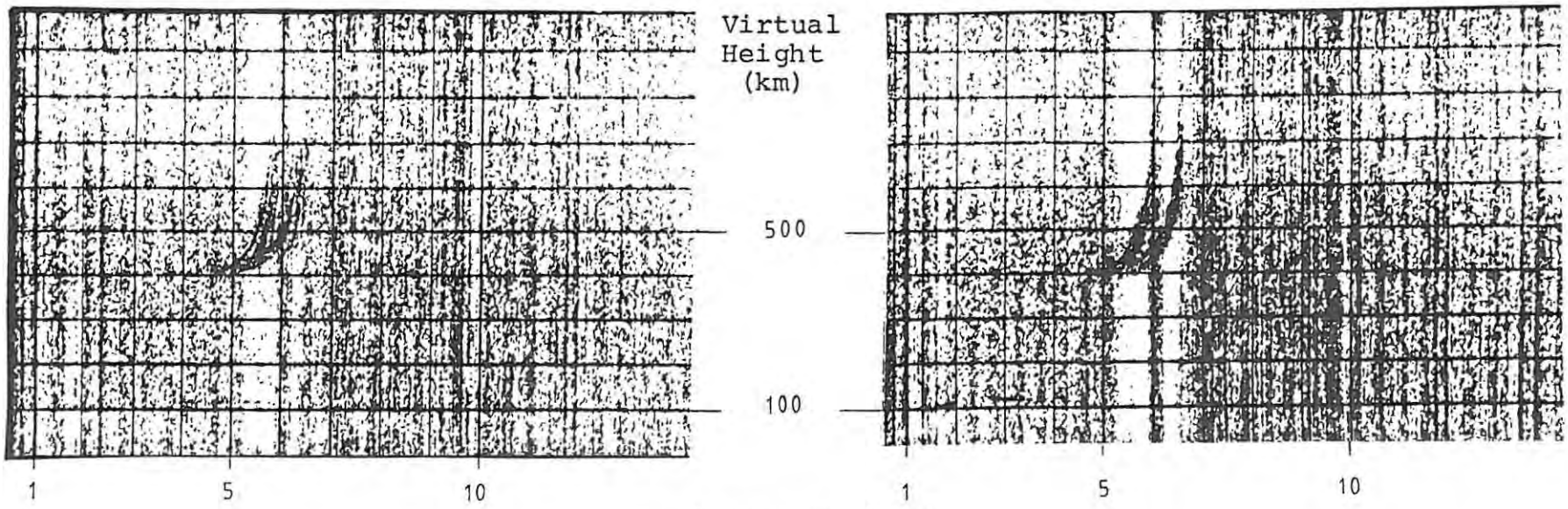

19:00UT 14th December,1978 - day 348 - SANAE 19:45UT

Figure 3.8

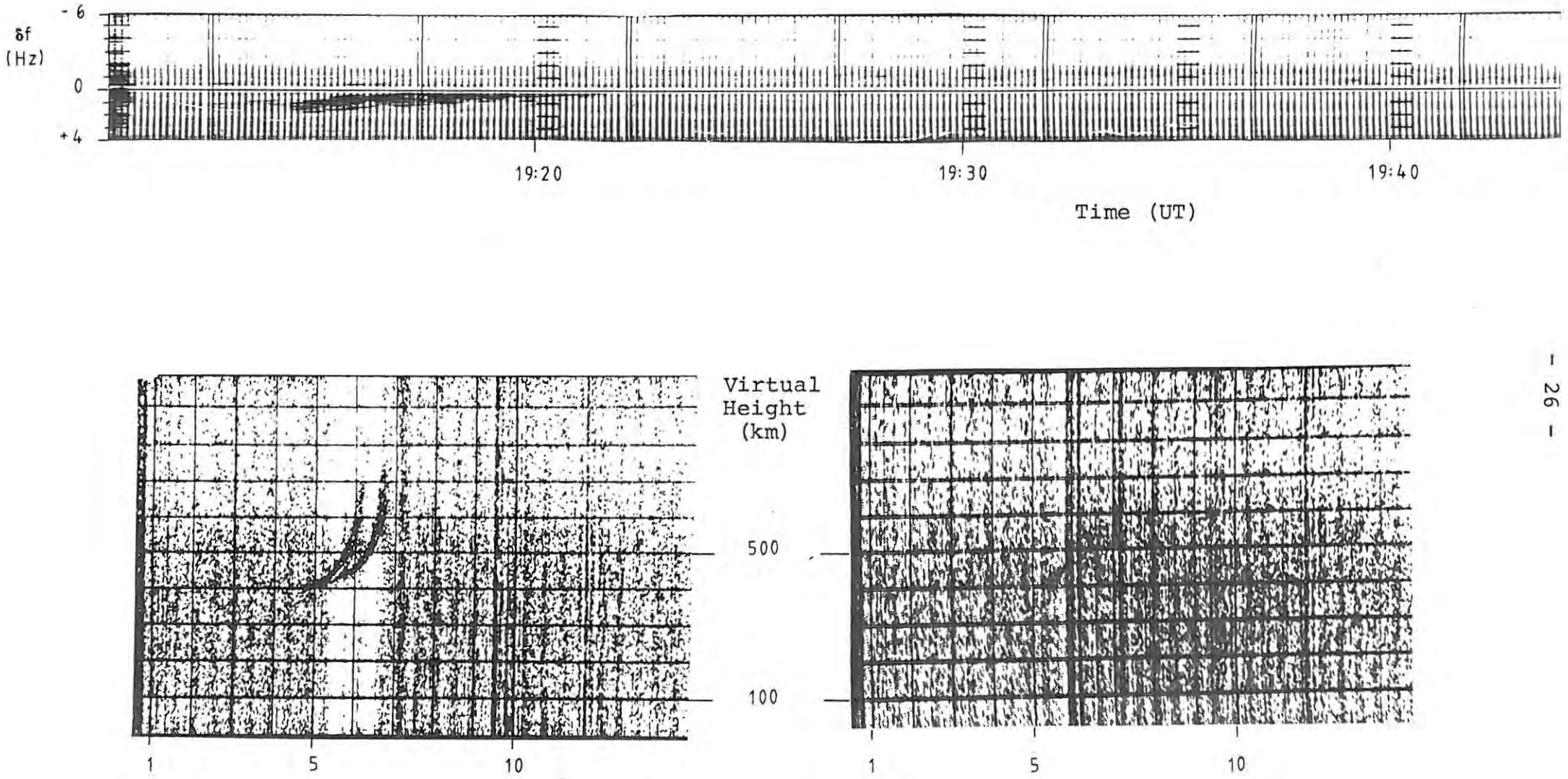
- 6
δf
(Hz)
0
+ 4
19:20
19:30
19:40
Time (UT)
Virtual
Height
(km)
500
100
1
5
10
1
5
10
Frequency (MHz)
19:00UT
15th December, 1978 - day 349 - SANAE
19:45UT

Figure 3.9

CHAPTER 4

THEORETICAL CONSIDERATIONS

4.1 Instrumentation Theory

It is instructive to derive an expression for the Doppler shift of a radio wave, in terms of the phase path length, and then to use FM theory together with Fourier Analysis theory to observe how the basic spectrum is affected by changes in the parameters.

Let the transmitted signal have the form

$$Y_T(t) = A_T(t) \text{ Cos } (\omega_c t) \quad , \qquad 4.1$$

where ω_c is the angular frequency (carrier) and is constant, and the phase constant is assumed to be zero.
After reflection from the ionosphere, the signal received has the form

$$Y_R(t) = A_R(t) \text{ Cos } (\omega_c t + \phi(t)), \qquad 4.2$$

where $\phi(t)$ is the phase difference between the transmitted and received signals and has a form dependent on the ionospheric parameters. This function is essentially arbitrary at this stage.

This received signal is mixed with a local oscillator

$$y_L(t) = A_L \text{ Cos } (\omega_L t) \quad , \qquad 4.3$$

to produce a signal

$$\tfrac{1}{2}A_R(t)A_L\text{Cos } \{(\omega_c+\omega_L)t+\phi(t)\} + \tfrac{1}{2}A_R(t)A_L\text{Cos } \{(\omega_L-\omega_c) - \phi(t)\} \; . \qquad 4.4$$

The first term of equation 4.4 can be removed by filtering and if we let

$$\omega_o = \omega_L-\omega_c \quad , \text{ (the offset frequency)} \qquad 4.5$$

and

$$A_s(t) = \tfrac{1}{2}A_R(t)A_L \quad ,$$

then the signal passed to the spectrum analyser is

$$V_s(t) = A_s(t) \text{ Cos } \{\omega_o t - \phi(t) \} \; . \qquad 4.6$$

$V_s(t)$ is a frequency modulated (FM) signal, with instantaneous frequency ω given by (from FM theory)

$$\omega = \omega_o - \frac{d\phi(t)}{dt} \quad , \qquad 4.7$$

and the modulating function is $\frac{d\phi(t)}{dt}$.

The phase difference between the transmitted and received signals can be expressed as a path length using

$$P(t) = \frac{\phi(t)}{k_c} \qquad 4.8$$

where k_c is the wavenumber $(= \frac{2\pi}{\lambda_c})$,
P is the phase path length,
λ_c is the free space wavelength and
$f_c \lambda_c = c$ (speed of light in vacuo).

This enables us to relate changes in phase to changes in ionospheric parameters, since the phase path length can be related to these as will be shown in section 4.2 of this chapter.

Equation 4.7 can be rewritten, in terms of P, as

$$\omega = \omega_o - \frac{2\pi f_c}{c} \frac{dP}{dt} \qquad 4.9$$

or, on dividing by 2π and rearranging,

$$f - f_o = - \frac{f_c}{c} \frac{dP}{dt} \qquad 4.10$$

The difference frequency, $f - f_o$, is usually called the Doppler shift, δf and it can be seen from equation 4.10 that the Doppler shift is proportional to the time rate of change of phase path length.

In order to monitor the Doppler frequency variations over a period of time, the Doppler signal is required in the

frequency domain, so that a Fourier transform of the time series is necessary. This is usually achieved by sampling the signal over a period of time, the integration time τ , and then transforming the set of samples. This integration time determines the frequency resolution after the spectrum analysis, as is well known from Fourier transform theory - for an integration time τ , the frequency resolution limit will be $\frac{1}{\tau}$.

For the Doppler case, the signal that is being transformed is expressed in general by equation 4.6 and is an FM signal if the amplitude is assumed to be constant. If the modulating function is slowly varying so that it does not change much during the integration time, equation 4.7 predicts that only a single frequency will be observed - the instantaneous frequency. This will be observed as a shift in the carrier frequency. On the other hand, if the modulating function varies fairly rapidly during the integration time, the observed spectrum can be fairly complex, depending on the modulating function. FM theory predicts that the carrier will have sidebands separated from it by the frequency of the modulating function and multiples of this frequency (assuming a sinusoidal modulating function). The number of significant sidebands is dependent on the amplitude of the modulating function and the amplitude distribution of the sidebands depends on the power spectral density distribution of the modulating waveform.

If the amplitude of the signal does not remain constant during the integration time, but varies in an arbitrary manner,

the final spectrum will be a convolution of the transform of the amplitude function and the FM spectrum. The less the amplitude varies during the integration time, the less effect its variation will have on the spectrum. How each of the terms in equation 4.6 affects the final spectrum can be seen by the following expression, where an asterisk is used to denote the operation of convolution,

$$v_s(f) = g(f) * a_s(f) * \frac{\mathrm{Sin}(\pi\tau f)}{\pi f} , \qquad 4.11$$

where g (f) is the Fourier transform of Cos $(\omega_o t - \phi(t))$,

$a_s(f)$ is the transform of $A_s(t)$,

and the factor $\frac{\mathrm{Sin}(\pi\tau f)}{\pi f}$ results from transforming a part, duration τ, of the time series.

The effect of $a_s(f)$ on the spectrum g(f) is not known since the form of $A_s(t)$ is dependent on the properties of the ionosphere at the time of sounding, but in most cases it is assumed to have little effect.

The discussion so far has had an underlying assumption that $\phi(t)$ is a single valued and continuously varying function. This is often unrealistic when ionospheric work is considered as it is possible to have reflections from tilted off-vertical regions of the ionosphere at the same time as reflections are being received from overhead regions. The above theory applies to a single reflector and the Doppler shift is a measure of the rate of change of phase path to this reflector.

If the theory is to be extended to include a number of individual reflectors, the simplest way is to assume that signals from the reflectors are summed on the antenna and that each reflector behaves as the single reflector discussed above. In this case the received signal (equation 4.2) becomes,

$$y_R(t) = \sum_j A_{R_j}(t) \text{ Cos } (\omega_c t + \phi_j(t)) \qquad 4.12$$

and all the operations involved in deriving equation 4.6 from equation 4.2 can be applied to each term in equation 4.12 (and the results summed) since the operations are linear, to produce,

$$V_s(t) = \sum_j A_{s_j}(t) \text{ Cos } \{\omega_o t - \phi_j(t)\} \qquad 4.13$$

and the equivalent of equation 4.11 is

$$v_s(f) = \frac{\text{Sin}(\pi \tau f)}{\pi f} * \{ \sum_j g_j(f) * a_s(f) \}. \qquad 4.14$$

The effect of a number of reflectors is seen to superpose the spectrum of each signal to produce a complicated spectrum, which explains why Doppler records are often very difficult to interpret.

It should also be mentioned that the signal being spectrum analysed must be bandlimited if aliasing is to be avoided in the frequency domain. This is best ensured by filtering the signal before spectrum analysis to be certain that high frequencies (above the spectrum analysis range) do not appear as low frequencies in the final spectrum.

The choice of integration time or spectrum analysis "window" is determined by a play-off between two factors. The time must be long enough to allow the spectrum to appear and short enough so that it does not change very much during the time. Afraimovich et al (1978) used a period of 37.5 seconds and claimed that this period does not contradict the available data or recommendations proposed by Mirkotan and Kushnerevskii (1964) regarding the choice of integration time. Integration time is not often mentioned in the literature but can usually be inferred from the resolution claimed. Integration times of the order of 10 seconds appear to be most commonly used.

It is essential to use the "overlapping window" or "instantaneous spectrum" method when very long integration times are used in order to obtain better time resolution of the spectrum.

For the chirpsounder, the integration time was 40 seconds during all the recording periods. Shorter integration times were not used as resolution was considered to be important in this initial study.

4.2 Doppler Theory

4.2.1. Ray Theory and Doppler Frequency Shifts

In the previous section, the Doppler shift was related

to the time rate of change of phase path by

$$\delta f = -\frac{f_c}{c}\frac{dP}{dt} \quad , \qquad 4.15$$

and mention was made that this could be used to relate the Doppler shift to changes in ionospheric parameters. A number of papers has been published which discuss this; in particular those of Bennet (1967a,1968) and Kelso (1960,1961) are worth mentioning. In order to simplify the mathematics it is necessary to make some assumptions about the nature of the ionosphere. Depending on the assumptions made, the model is usually classified as isotropic and homogeneous, or the converse of one or both of these terms.

The ionosphere is assumed to be slowly varying and collisions are neglected (lossless medium). The earth's magnetic field is included and the phase refractive index, μ, is assumed to be finite and non-negative. The phase path must be greater than several wavelengths and the phase path is assumed not to change greatly during one cycle of transmitted frequency. The phase path is assumed not to change much during the time of flight of an element of the wave, and the Doppler shift is assumed to be small compared to the transmitted frequency. Bennet (1968) has given a more rigorous and mathematical statement of the above assumptions.

The phase path P can be defined by

$$P = \int_{A(t)}^{B(t)} \bar{\mu}.d\bar{s}, \qquad , \qquad 4.16$$

where A(t) and B(t) are the endpoints of the path not fixed in general,

$\bar{\mu}$ is a vector in the direction of the wavenormal and of magnitude equal to the phase refractive index,

and $d\bar{s}$ is a directed segment of the ray path.

If we use a general coordinate system with coordinates x_1, x_2, x_3 and write equation 4.16 in tensor notation, using the summation convention over the 3 components,

$$P = \int_{A(t)}^{B(t)} \mu_i \, dx_i \qquad . \qquad 4.17$$

Fermat's principle states that the optical path length, as defined by 4.17 of an actual ray between two points, is shorter than the optical path length of any other curve which joins these points and which lies in a certain regular neighbourhood of it. The principle can be stated in the notation of the calculus of variations as

$$\delta \int_{A(t)}^{B(t)} \mu_i \, dx_i = 0 \qquad , \qquad 4.18$$

that is, the first variation of the phase path with respect to variations of the path is zero.

Equation 4.17 can be rewritten as

$$P = \int_{u_1(t)}^{u_2(t)} \mu_i \frac{dx_i}{du} \, du \quad , \qquad 4.19$$

where u is an aribtrary monotonically increasing parameter. It is convenient to define a function $F(x_i, \dot{x}_i, t)$ by

$$F = \mu_i \frac{dx_i}{du} \quad , \qquad 4.20$$

where a dot denotes differentiation with respect to u. Equation 4.19 becomes

$$P = \int_{u_1(t)}^{u_2(t)} F \, du \quad , \qquad 4.21$$

and Fermat's principle implies (see Appendix 2) that

$$\int_{u_1(t)}^{u_2(t)} \left\{ \frac{\partial F}{\partial x_i} \eta_i + \frac{\partial F}{\partial \dot{x}_i} \dot{\eta}_i \right\} du = 0, \qquad 4.22$$

where the η_i are arbitrary differentiable functions that vanish at the endpoints $u_1(t)$ and $u_2(t)$.

Differentiation of equation 4.21 yields

$$\frac{dP}{dt} = \int_{u_1(t)}^{u_2(t)} \frac{\partial F}{\partial t} \, du + F(x_i, \dot{x}_i, t) \Big|_{u=u_2(t)} \frac{du_2(t)}{dt} - F(x_i, \dot{x}_i, t) \Big|_{u=u_1(t)} \frac{du_1(t)}{dt} \qquad 4.23$$

where it is essential to remeber that both endpoints are time dependent. A discussion of the differentiation of an integral

with variable endpoints can be found in texts on advanced calculus such as Lee (1972).

Evaluation of the first term of 4.23 is done using the chain rule to give,

$$\frac{\partial F}{\partial t} = \frac{\partial F}{\partial \mu}\frac{\partial \mu_i}{\partial t} + \frac{\partial F}{\partial x_i}\frac{\partial x_i}{\partial t} + \frac{\partial F}{\partial \dot{x}_i}\frac{\partial \dot{x}_i}{\partial t}$$

and using 4.20 simplifies this still further to

$$\frac{\partial F}{\partial t} = \dot{x}_i \frac{\partial \mu_i}{\partial t} + \frac{\partial F}{\partial x_i}\frac{\partial x_i}{\partial t} + \frac{\partial F}{\partial \dot{x}_i}\frac{\partial \dot{x}_i}{\partial t} \quad . \qquad 4.24$$

Comparisons of the last two terms of this expression with the R.H.S. of equation 4.22 shows that their contribution to the integral will be zero as a special case of 4.22 with $\eta_i = \frac{\partial x_i}{\partial t}$. For this particular integral, $u_2(t)$ and $u_1(t)$ can be considered to be fixed because each ray can be characterized by a single value of t (Bennet 1968) and thus η_i will vanish at the endpoints as required. Although we have evaluated $u_2(t)$ and $u_1(t)$ at the time characteristic of the ray under consideration it is important to remember that the endpoints are in fact moving and thus have an instantaneous velocity at that time. Combining 4.24, 4.23 and the special case of 4.22 yields

$$\frac{dP}{dt} = \int_{u_1(t)}^{u_2(t)} x_i \frac{\partial \mu_i}{\partial t} du + F\Big|_{u=u_2(t)} \frac{du_2}{dt} - F\Big|_{u=u_1(t)} \frac{du_1}{dt}$$

$$= \int_{u_1(t)}^{u_2(t)} \frac{\partial \mu_i}{\partial t} \frac{dx_i}{du} du + \mu_i \frac{dx_i}{du}\Big|_{u=u_2(t)} \frac{du_2}{dt} - \mu_i \frac{dx_i}{du}\Big|_{u=u_1(t)} \frac{du_1}{dt}$$

$$= \int_{u_1(t)}^{u_2(t)} \frac{\partial \mu_i}{\partial t} dx_i + \mu_i \frac{dx_i}{dt}\Big|_{x=B} - \mu_i \frac{dx_i}{dt}\Big|_{x=A}$$

$$= \int_{u_1(t)}^{u_2(t)} \frac{\partial \bar{\mu}}{\partial t} \cdot d\bar{s} + [\bar{\mu}.\bar{v}]_B - [\mu.\bar{v}]_A \quad . \qquad 4.25$$

If the angle between the wavenormal and the ray direction is α then equation 4.25 can be written

$$\frac{dP}{dt} = \int_{u_1(t)}^{u_2(t)} \frac{\partial \mu}{\partial t} \cos \alpha \, ds + [\bar{\mu}.\bar{v}]_B - [\mu.\bar{v}]_A . \qquad 4.26$$

This result is not unexpected since it is exactly what the calculus of variations predicts for a problem when both the integral and limits vary. There are two contributions, one from the variation of the integral and one from the variation of the endpoints. As applied in this particular case, the phase path has contributions due to changes in the refractive index over the ray path associated with the particular value of t under consideration and a contribution due to the instantaneous velocity of the endpoints at the same time t. The Doppler shift can be evaluated by using equation 4.15.

The Doppler shift observed can be associated with changes in refractive index (as a result of redistribution

of ionization in the ionosphere), or movements of the reflection level (as a result of bulk movements of, or within, the ionosphere). If the transmitter and receiver are fixed points on the earth, the ray path is divided into two parts, one from transmitter to reflection point and one from reflection point to the receiver. This is necessary to ensure continuity of the derivatives when Fermat's principle is applied.

The result 4.26 has been derived by some authors including Bennet (1968) and special cases of it by Kelso (1960), Kimura and Nishina (1967) and Bennet (1967a). In most cases, the method used differs from that given above, although all the papers quoted make use of Fermat's principle and differ only in the method of obtaining the final result. Kelso derives the result for an inhomogeneous quasi-isotropic ionosphere when the transmitter is moving and the receiver is stationary. Kimura et al (1967) extended Kelso's treatment to the anisotropic case, using the same method. Bennett (1968) uses Hamilton's optical method in addition to Fermat's principle to derive the result for the inhomogeneous anisotropic case and allowing both endpoints to move.

The derivation leading to equation 4.26 only makes use of Fermat's principle and derives the result using only the calculus of variations as it applies to an integral with varying endpoints (Fox (1963)). The result applies to the inhomogeneous, anisotropic case and has the advantage that it does not require the introduction of a colour index, as required if Hamilton's

optical method is used. This simplifies the algebraic manipulation in obtaining the result.

Kelso (1960) applied the result to the case of a satellite transmitting to a receiving station on the ground and in a later paper (1961) considers the case of two signals being transmitted from the satellite.

Dyson (1975) uses equation 4.26 to discuss the relationship between angle of arrival and Doppler shift and indicates how, using two different frequencies (or ordinary and extraordinary components of one frequency) and measuring both angle of arrival and Doppler shifts,it is possible to determine whether the Doppler shift is due to time changes of the refractive index along the ray paths or to bulk motions of the medium. Distinguishing between the two different contributions is important in interpretation of the Doppler records.

4.2.2. Corrugated reflector model

If the Doppler shift is due to bulk motions only, the theory can be simplified, as the reflecting layer acts as a corrugated reflector and the Doppler shift can be determined in terms of movements of this reflector.

A summary of some of the theory associated with a corrugated reflector as it applies to the vertical incidence case is given below.

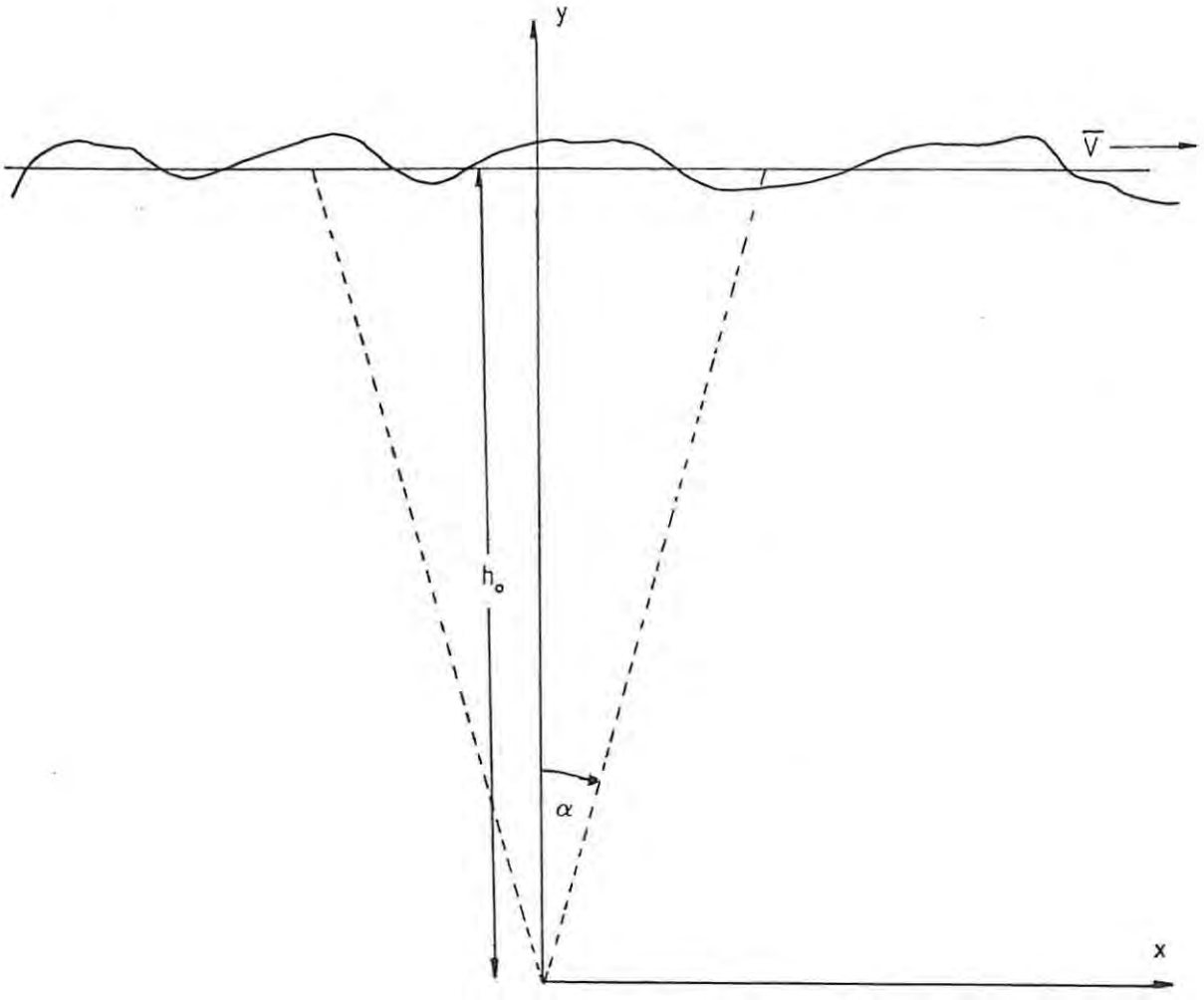

Figure 4.1

Coordinate System used for Corrugated reflector model

Reflection is assumed to take place at a corrugated horizontal surface of equal electron density at a height h_o above the earth. The coordinate system is chosen so that the transmitter is at the origin and the x-axis is in the direction

of the wavenormal of the perturbing wave. The y-axis is chosen to be vertically upwards. The energy radiated from the transmitter is assumed to be directed within an angle α from the y-axis. The velocity of the perturbing wave is assumed to have magnitude v. The reflector can be expressed as

$$y(x,t) = h_o + g(x-vt) \quad , \qquad 4.27$$

where g(x) is an arbitrary, differential function. Differentiation of equation 4.27 with respect to x leads to

$$\frac{\partial y}{\partial x}(x,t) = \frac{dg}{dx}(x-vt) \quad . \qquad 4.28$$

The reflection process is assumed to be "mirror reflection" so that for energy to be returned to the transmitter, the ray must meet the reflector at right angles (the rays are assumed to be straight lines between transmitter and reflector, i.e. free space below the reflector). Figure 4.2 shows the geometry of such a reflection and from this it can be seen that the angle, θ, between the ray and the y-axis, in a positive sense can be expressed as

$$\theta(x_r,t) = - \arctan \left(\frac{\partial y}{\partial x}(x_r,t) \right) ,$$

or

$$\theta(x_r,t) = - \arctan \left(\frac{dg}{dx}(x_r-vt) \right) , \qquad 4.29$$

where a subscript r is used to indicate a reflection of the type described above.

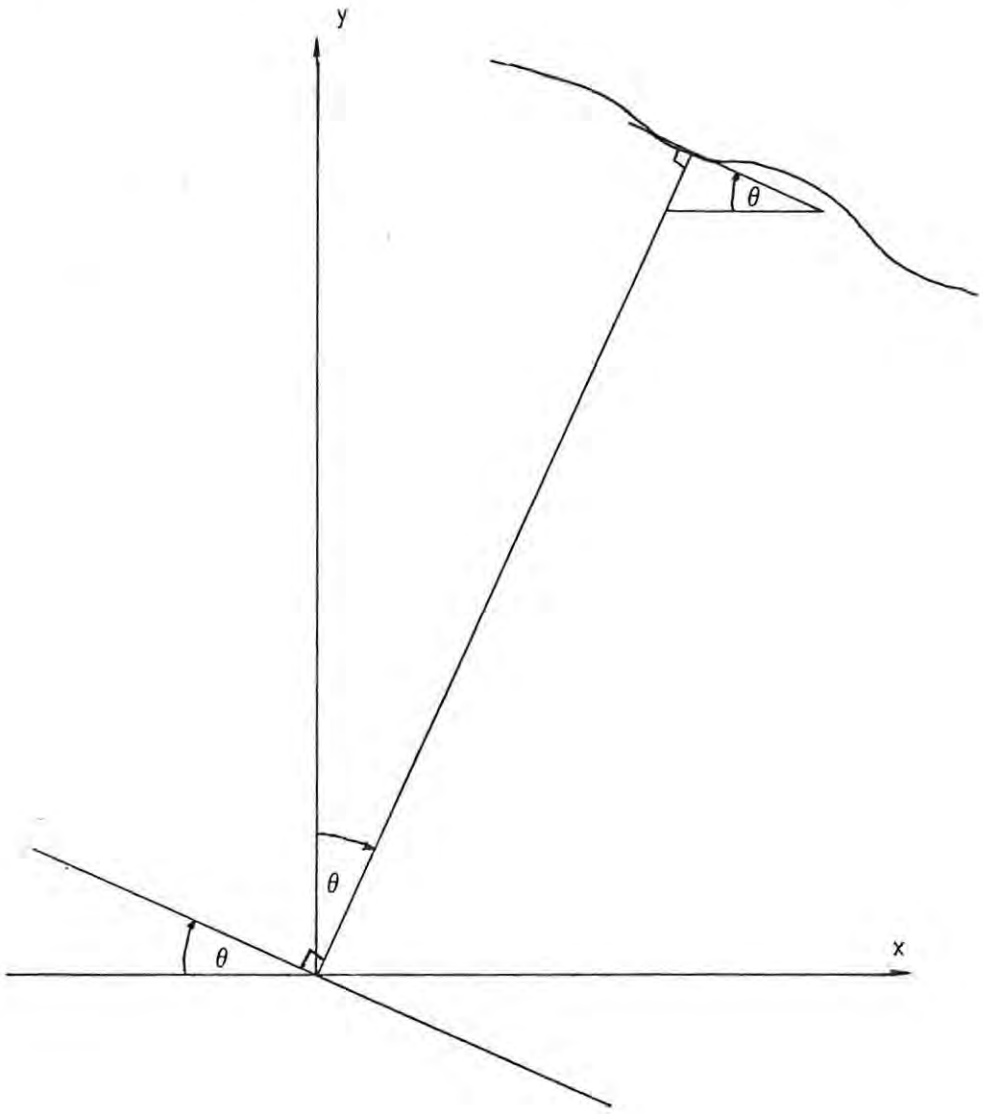

Figure 4.2

Geometry of a reflection

The Doppler shift can be expressed as

$$\delta f = -\frac{2f}{c} v \sin\theta \quad , \qquad 4.30$$

where values of θ that are greater than α in magnitude will

not be observed as they will be outside the beam of the antenna. Combining equations 4.30 and 4.29 gives

$$\delta f = -\frac{2f}{c} v \operatorname{Sin} \left\{ \arctan \left(\frac{dg(x_r - vt)}{dx} \right) \right\} \qquad 4.31$$

with the conditions

$$-h_o \tan | \alpha | \leq x_r \leq h_o \tan | \alpha | \quad , \qquad 4.32$$

and

$$\left| \frac{dg(x_r - vt)}{dx} \right| \leq \tan | \alpha | \quad . \qquad 4.33$$

It is possible for reflections to occur from more than one angle at a time and thus give rise to a multivalued Doppler curve under certain conditions.

As an example, consider the case of a sinusoidal reflector moving with a velocity v in the positive x direction. The equation of the reflector is

$$g(x) = A \operatorname{Cos} \left(\frac{2\pi x}{\lambda} \right) \qquad 4.34$$

and the resulting Doppler shift is plotted in Figure 4.3 for two cases.

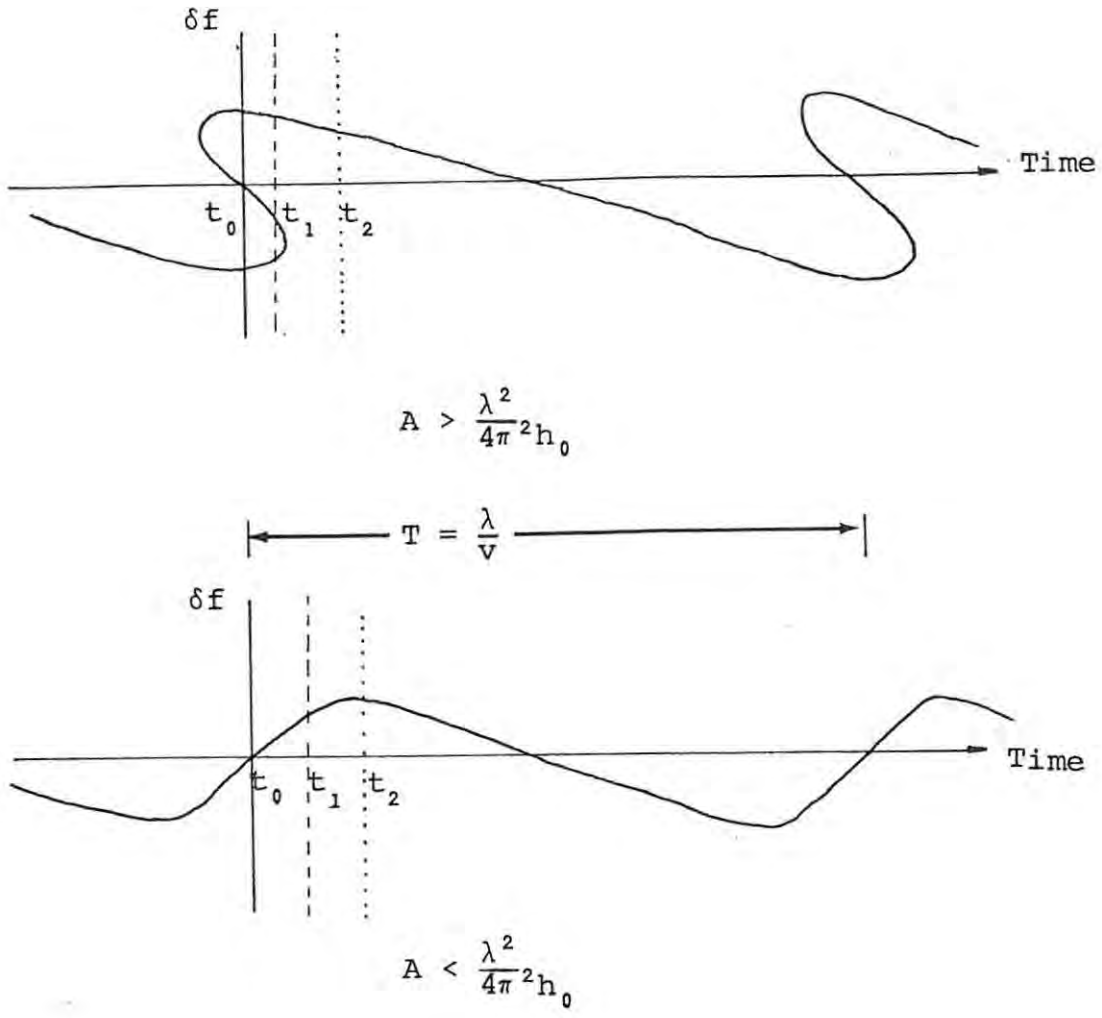

Figure 4.3

Doppler shifts from a Sinusoidal Reflecting Surface

Note that under certain conditions, the curve folds back on itself and multiple reflections occur. The foldback occurs when the maximum of the sinusoid is over the origin and provided that the radius of curvature at that point is larger than h_o, the height above the transmitter. Thus multiple reflections occur if

$$A > 4\pi^2 \frac{\lambda^2}{h_o} \quad . \qquad 4.35$$

Ray diagrams for the two cases are shown in Figure 4.4 .

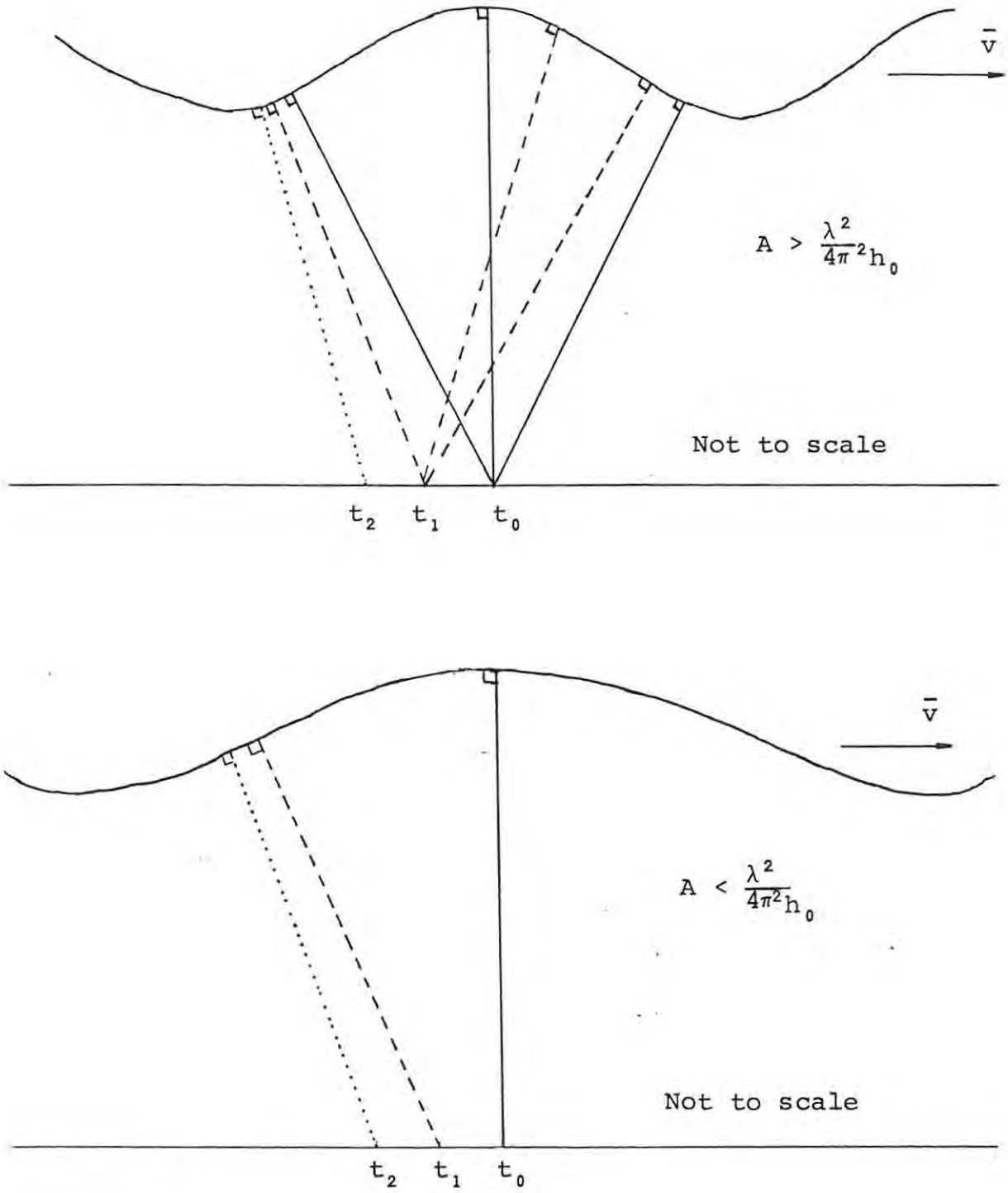

Figure 4.4

Ray diagrams of reflections from a sinusoidal reflector

Rays are shown for three different times (the layer is shown stationary while the transmitter is moved below in the opposite direction producing the same result as a moving layer). The solid lines correspond to the zero of time in Figure 4.3 and the dashed and dotted lines are the ray positions at later times. The approximate times on the Doppler shift curves are indicated by similar dashed and dotted lines.

For the case $A < \frac{\lambda^2}{4\pi^2 h_o}$, the locus of the reflection point can be shown to be an ellipse as the reflector moves overhead.

Lyon (1979) deals with a corrugated reflector model for one-hop oblique propagation and compares the results of the Doppler records over the Ottawa to London path, with the predictions of the model. Some reports of the characteristic "S" shaped curve associated with the sinusoidal reflector have appeared in the literature (e.g. Davies and Baker (1966)), but it appears that in most cases the Doppler shift consists of contributions from bulk motions and from variations of the refractive index along the ray path, making interpretation of the records difficult.

The corrugated reflector has been successfully used by Bowman (1960 a,b) to explain range and frequency spreading on ionograms. Cornelius and Essex (1979) make mention of the fact that, provided the wavelength of the ripple is small enough, the Doppler spectrum appears to be unstructured. In

the theory presented above the wavelength has been considered to be large so that reflections only occur from overhead or near overhead regions. Under certain conditions multiple reflections (3 in the above case) could occur. If the wavelength of the reflector (assumed sinusoidal) is reduced, it is possible to obtain reflections from fairly large off vertical angles. Figure 4.5 shows the ray diagram for a case of this type.

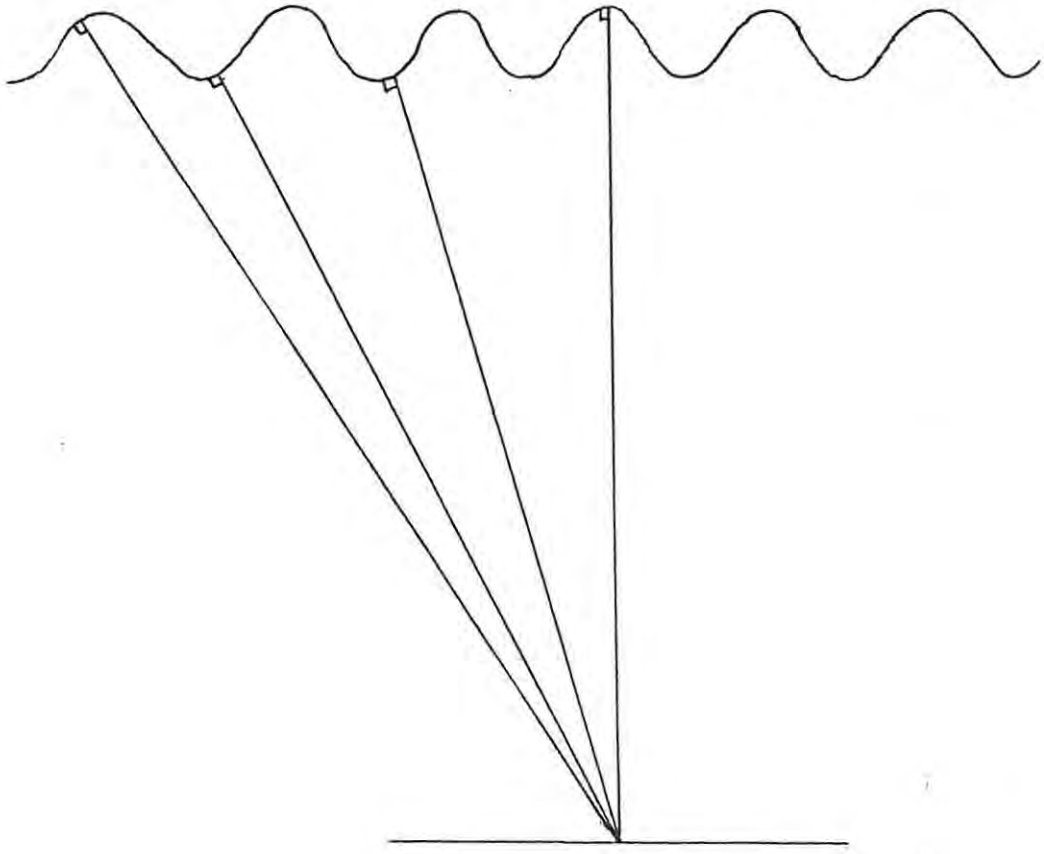

Figure 4.5
Ray diagram for multiple reflections from sinusoidal layer

Results have been obtained for a case of this type by Cornelius and Essex (1979a) where twenty-five multiple reflections were

received from a sinusoidal contour with an amplitude of 3km and a wavelength of 30km, travelling with a speed of 100 m/s. The resulting Doppler record is unstructured and the extent of this is determined by the amplitude to wavelength ratio. The effect of small ripples on the sinusoidal contour would be to produce fading of the signals and result in an even more unstructured Doppler trace.

4.3 Geophysical theory associated with Doppler shifts

A survey of the literature shows that a large number of "Doppler events" are associated with certain geophysical phenomena and a number of papers have been devoted to the theoretical understanding of these events.

4.3.1. Solar flares

The term "sudden frequency deviation" (sometimes abbreviated to SFD) was proposed by Chan and Villard (1963) for the ionospheric perturbations, that are manifested in the form of sudden frequency deviations on Doppler records, during solar flares. First x-ray radiation and hard ultra-violet radiation during solar flares are thought to cause the perturbations. A large number of papers have been devoted

to the subject of SFD's, for example Davies and Baker (1966), Chan and Villard (1963), Kanellakos, Chan and Villard (1962) and Namazov et al (1976), to name a few.

Davies and Donnelly (1966) suggest that the SFD is associated with the explosive phase of the H_α flare. This phase is the short period during which there is rapid expansion of the H_α flare borders and there seems to be a good correlation between the times of SFD's and times of these phases of flares. Difficulties associated with the detection of the explosive phase of small flares and the detection of SFD's at times of sunrise and sunset make it difficult to determine whether all explosive phases are associated with SFD's. With respect to duration, recovery time constant, time of maximum and height of enhanced ionization, SFD's are distinguished from other flare-associated ionospheric effects on radio waves (Chan and Villard(1963)). In particular, it is interesting to note that the height of enhanced ionization producing SFD's is thought to be that of the E - F_1 region (between 120 - 200 km). This result was obtained by Chan and Villard (1963) and also by Kanellakos, Chan and Villard (1962) and Kanellakos and Villard (1962), from the recombination time constant of the enhanced ionization and the change in absorption of the received signal. Reports indicate that the initial ionization may or may not be followed by ionization in the D region, resulting in loss of signal as a result of absorption.

The results suggest that solar flares produce ionization in the upper E - lower F_1 region and that the SFD observed on Doppler records is as a result of this enhanced ionization rather than variations in the height of reflection. The expression for the Doppler shift can thus be written as

$$\delta f = - \frac{2f_c}{c} \int_o^h \frac{\partial \mu}{\partial t} \text{ Cos } \alpha \, ds$$

where the variables have the same meanings as in equation 4.10 and 4.26 and the vertical incidence case has been considered. By neglecting collisions and the magnetic field and using an expression for μ derived from the Appelton-Hartree equation, it is possible to relate changes in μ to changes in the electron density, N, and thus relate the Doppler shift to changes in N in the region of enhanced ionization. This is done by Chan and Villard (1963), for example.

4.3.2. Magnetic Field Variations

Changes in the Doppler frequency correlating with changes in the magnetic field have been reported in the literature from time to time and by a number of groups. In particular there is an association between Doppler shifts and magnetic sudden commencements, micropulsations, sudden impulses and magnetic storms. Of these, the correlation with

a storm sudden commencement (ssc) is the most often reported correlation. The papers of Jacobs and Watanabe (1966), Huang et al (1973), Ichinose and Ogawa (1974) and Huang (1976), in addition to that of Davies and Baker (1966), referred to in the section on solar flares, are worth mention in this regard.

Unlike the SFD's associated with solar flares, a sudden commencement has an effect that can be observed either during the day or at night. The form of the Doppler variation is usually more complex in this case and can usually be broken down into a number of parts, namely a large positive or negative (or both) peak followed by almost sinusoidal "ringing". Often correlations are observed between one of the components of the magnetic field and the Doppler variation, as for example by Davies and Baker (1966) and Huang et al (1973) where correlations were observed between the Doppler records and the D and H magnetic components respectively.

Similar correlations have been reported in the case of magnetic micropulsations by Chan et al (1962) and in the case of a magnetic sudden impulse by Kanellakos et al (1962).

As with solar flare effects on Doppler records, a notation has been introduced to classify the effects of sudden commencements as they are observed on the Doppler records. The notation follows a similar convention to that introduced by Akasofu and Chapman (1959) for sudden commencements as observed

on the H component of the magnetic field. The notation for Doppler effects is to classify as one of SCF(+); SCF(-); SCF(+-) or SCF(-+), depending whether the record shows a single positive, negative, positive followed by negative or negative followed by positive peak, respectively, at the time of the sudden commencement.

Work on the phase relationship between sudden commencements and the Doppler fluctuations has been reported by Chan et al (1962), Huang et al (1973) and Ichinose and Ogawa (1974). Theory connecting Doppler shift and geomagnetic variation has been reported by Rishbeth and Garriott (1964), Jacobs and Watanabe (1966) and extended by Huang (1976).

It should be noted that the effect of a sudden commencement may cause a change in the refractive index or a change in the ray path as a result of changes in the magnetic field or changes in the distribution of electrons and ions as a result of electric fields associated with the changing magnetic field. The problem of determining the causes in individual cases is difficult and the problem is in general a very complex one. Theory concentrates on a particular set of assumptions concerning the causes and cannot always be expected to result in excellent correlation with the data.

4.3.3. Earthquakes and Nuclear Explosions

There have been reports in the literature indicating that Doppler shifts have been observed during earthquakes (Yuen, Weaver,Suzuki and Furimoto (1969)) and at times of nuclear explosions (Baker and Davies (1968)). Earthquakes are known to be sources of acoustic waves and these can be observed as they propagate to ionospheric altitudes and distort iso-ionic contours in the process. Similar acoustic waves can be produced at times of nuclear explosions and observed at ionospheric altitudes using the HF Doppler technique. Both gravitational waves and acoustic waves will be discussed in the next section, under the general heading Atmospheric Waves.

4.3.4. Atmospheric Waves

Wavelike phenomena in the atmosphere have been studied by a number of groups using a variety of techniques. Special interest has been shown in the effect on the ionosphere of waves in the neutral atmosphere. The reader is referred to the Symposium on Upper Atmospheric Winds, Waves and Ionospheric Drifts held at St. Gallen, Switzerland in 1967. The papers presented at that symposium cover a wide range of topics related to Atmospheric Waves and are

contained in number 5 of J. Atmos. Terr. Phys. 30 (1968) 657-1063. Reference will be made to some of the individual papers contained in that number, later in this section.

For the purpose of study, atmospheric waves can be divided into two types - low frequency gravitational waves and high frequency acoustic waves. Although these waves may start as pressure variations in the neutral atmosphere (as a result of an earthquake, for example), the ionized gas in the upper atmosphere is also set in motion and iso-ionic contours become distorted as the wave propagates. Nelson (1968) presents theory associated with the response of the ionosphere to these waves. The characteristics of the waves are obviously dependent on the source as well as on variations and properties of the medium through which they propagate. It could be expected that the variations observed at ionospheric heights do not correspond exactly to pressure variations measured on the earth but would be related to these, to winds in the upper atmosphere and to the earth's magnetic field in a fairly complex way. Hines (1968 b, 1968 c) discusses the effect of molecular dissipation and ohmic losses in gravity waves. Lomax and Nielson (1968) mention some observations showing geomagnetic field dependence.

Earthquakes and nuclear explosions have been mentioned as possible sources of acoustic waves, but these are by no means the only sources of these waves. Severe storms and high winds in the troposphere, as well as the effect of land masses on

winds, have been suggested as possible sources of atmospheric waves propagating to ionospheric heights (e.g.Dudeney et al (1977)). Solar eclipses and other solar induced phenomena such as flares and ssc's are also thought to be associated with the generation of atmospheric waves (Ichinose and Ogawa (1976), Cornelius and Essex (1978)). The HF Doppler technique is a very powerful tool for observing these atmospheric waves as they propagate ionospheric heights, but interpretation can be made difficult by the complexity of the association with other geophysical phenomena.

Both acoustic waves and gravitational waves are limited in their propagation by atmospheric filtering which is dependent on the frequency of the waves. As a result there are cut-off frequencies outside of which propagation will not occur. Acoustic waves are limited from above by viscous damping and from below by a cut-off frequency, ω_a, the frequency at which the entire atmosphere will oscillate if compressed in the vertical direction and then released. Both these limits vary with height in the atmosphere (see Georges (1968) for a height-frequency plot for acoustic waves). For gravitational waves, the upper limit of frequency is the Brunt-Väisälä frequency, ω_g, the frequency at which a bounded volume of atmospheric air will oscillate after being displaced in the vertical direction.

The name "travelling ionospheric disturbance" (TID) has been given to gravitational waves propagating at ionospheric heights and a number of papers have appeared in the literature

reporting TID's. Lyon (1973), Georges (1968) and Chan and Villard (1962a) are examples where the HF Doppler technique has been used. Theoretical understanding of TID's, as well as the mechanism behind their production, are of importance if data are to be interpreted correctly. Francis (1974) discusses medium scale TID's from a theoretical point of view, as well as theory associated with their excitation by the Auroral electrojet. Results obtained for the period of gravity waves by the Doppler method agree with those obtained by other methods (Essex (1975)).

In order to predict the Doppler shift that will be observed as a TID moves over the recording station, use is often made of the corrugated reflector model discussed in section 2 of this chapter. The corrugated reflector is identified with the distorted iso-ionic contours during the passage of the wave. The ratio of the amplitude of the wave to its wavelength is important in determining the form of the Doppler record as multiple reflections occur when this ratio reaches a critical value and can result in an unstructured Doppler record if the ratio is large enough. Evidence for the distorted iso-ionic contours is given by Bowman (1968), Georges (1968), Hooke (1968), Baker and Gledhill (1965) and Bowman (1960 a,b). Toman (1976) suggests this interpretation of Doppler data and Cornelius and Essex (1975) present evidence for the existence of scattering irregularities in the mid-latitude ionosphere. These scatterers move with the background ionosphere during the passage of a TID and thus the Doppler data can be used to determine TID characteristics in this case as well.

4.3.5. Spread-F and Sporadic E

The occurrence of both range and frequency spread on ionograms may lead one to expect that these phenomena may be detected by means of a Doppler system as well and that it may be possible to understand the nature of "spread-F" as a result of these investigations. Cornelius and Essex (1979a) present some Doppler observations that were associated with spread-F on ionograms, and make some suggestions as to possible interpretation of the data. Bowman (1960 a, 1960 b) has shown how "spread-F" can be explained using a particular model of the processes involved and similar models have been used to predict the Doppler shift that may be expected under similar circumstances.

Movements of troughs of ionization in the ionosphere have been observed on ionograms - the mid-latitude trough is a familiar example. "Polar spur" is fairly often observed at high-latitude stations and is associated with movements of this mid-latitude trough. Using a sequence of ionograms, it is possible to determine the virtual range of the trough and to plot its movement from the time reflections are received from it and until reflections are no longer returned to the receiver. Doppler measurements would yield the line of sight velocity of the reflecting point and thus it is possible to have a position and velocity for the trough at a number of times. More accurate reconstruction of the path of the trough is thus possible.

Movements of the sporadic E layer have also been observed by means of Doppler sounders, for example Cornelius and Essex (1979 b). Moving clouds in the layer have been observed in this way and models allow information about sporadic E layers to be determined.

4.3.6. Concluding Remarks

Discussions presented in this section have shown that the HF Doppler technique is a very powerful tool for detecting movements of and within the ionosphere. The broad range of observable effects, associated with a variety of geophysical phenomena, is indicative of its usefulness in leading to a better understanding of these areas of solar terrestrial physics.

I have no doubt that, even though at present there is a certain amount of uncertainly in interpretation of the data, the HF Doppler technique will be one of the major contributors to knowledge in ionospheric physics (and ultimately in solar terrestial physics), in the near future.

CHAPTER 5

ANALYSIS AND INTERPRETATION OF THE DATA

5.1 Introduction

Examination of the solar and magnetic conditions prevailing at the time of recordings has revealed that some distinct "events" have been recorded during this initial study. Possibly the most interesting of these was the magnetic sudden commencement which occurred on 4th June, 1978. A solar flare was observed on 14th August and its effect on the Doppler record is described. The other data do not contain any known solar "events" but do show some general features that are instructive to analyse and to interpret.

The most striking features of the Doppler records shown in Chapter 3 are the numerous lines making up the traces in most cases. The length of the lines is, to a certain extent, determined by the spectrum analyser because of the long integration time used. This is because, even though the input signal is sampled at a 30 Hz rate and the memory updated accordingly, it takes a period of 40s for the contents of the memory to be completely replaced. Thus, frequencies which were in the input signal may still be present in the output spectrum after that component has ceased to be one of the input frequency components. The effect that this has is to produce a "smeared" spectrum (smeared in time and not in frequency) but it has the

advantage that frequency components appearing in the input signal are seen in the output signal fairly soon after this (the delay is as a result of a minimum energy level required to produce a signal on the oscilloscope and depends on the signal strength of the input component). This is illustrated in Figure 5.1 .

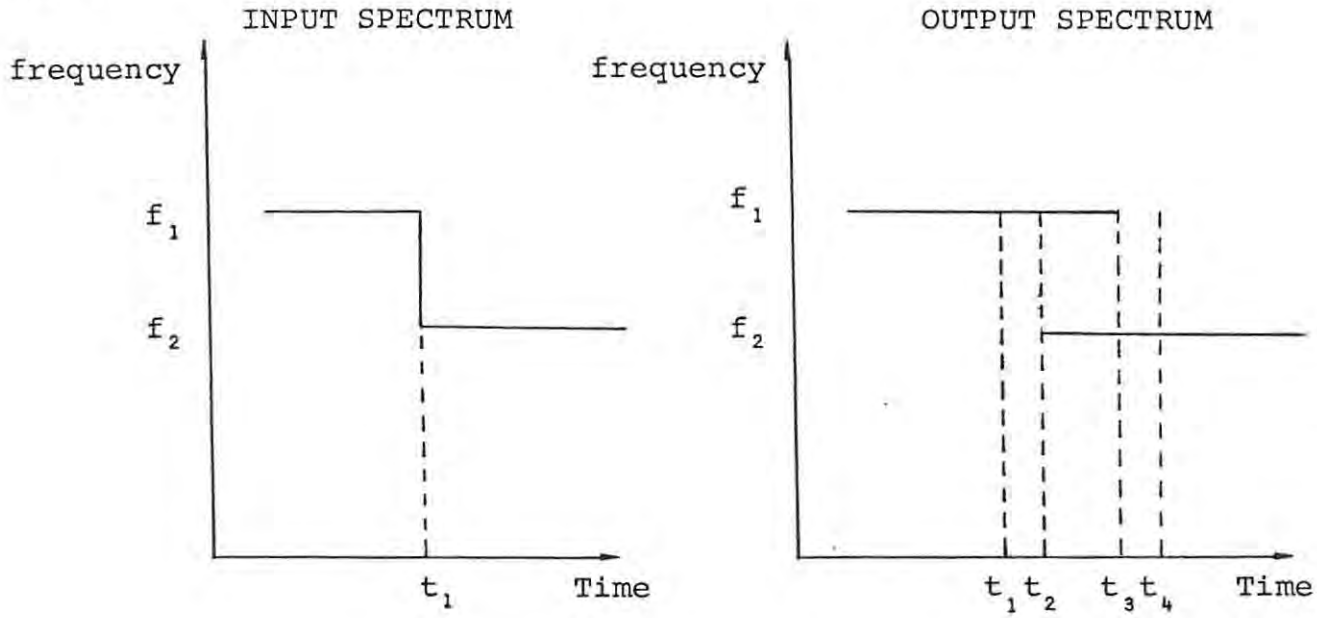

Figure 5.1

Smearing of the Spectrum

A signal generator was used to inject a signal of frequency f_1 into the spectrum analyser. At time t_1, the signal generator frequency was changed to f_2 and this appears in the output spectrum at time t_2 ($t_2-t_1 \sim 10$ seconds) while frequency f_1 remains in the output spectrum until time t_3. Time t_4 is chosen to be 40 seconds after t_1 (time at which

samples from f_1 are no longer present in the memory). The overlap time $(t_3-t_2)$was found to be of the order of 20 seconds and if it is assumed that

$$t_2-t_1 = t_4-t_3$$

then the build up time (t_2-t_1) is of the order of 10 seconds. The building time and hence the overlap time are dependent on the amplitude of the input signal.

Two more questions about the nature of the records can be asked. Firstly, why is there a blank region around the OHz line? Secondly, what is the mechanism that produces the frequencies represented by the lines in the record? The first question can once again be answered by looking into the instrumentation of the Chirpsounder. Use is made of a "crispener" in order to reduce the sidebands around a very strong signal and the effect of this is to remove any weak signals that may be present in this region. The OHz line is very strong as a result of RF leakage from the transmitter to the receiver. This signal is present at all times and thus has a blank region around it. The second question is more difficult to answer and the solution may or may not be found in the instrumentation. Extensive investigation of the equipment and method of spectrum analysis failed to produce any instrumental source of the lines as did suggestions such as interference from other radio stations. These investigations, theoretical as well as practical, of the

experimental method used, have led to the conclusion that the lines are a very real part of the Doppler spectrum and as a result are in need of explanation. This has recently been confirmed by Dudeney (1979, private communication), who has found that data recorded at Argentine Islands can be displayed in such a way as to show the fine structure and broad character of the trace, resulting in a record very similar in character to those shown in chapter 3. Some details of the tests conducted are contained in Appendix 3.

Analysis of the data will start with the sudden commencement and flare events, followed by an analysis of the remaining records.

5.2 Magnetic sudden commencement - 4th June, 1978 (day 155)

This sudden commencement was reported by an number of stations and the mean time from those reporting the ssc was 12:11 UT. Both the magnetograms and the micropulsation records at SANAE for that day indicate the ssc quite clearly and the Doppler record leaves one in no doubt that there was an SCF. Also very noticable on the Doppler record is the marked increase in the number of little lines making up the trace immediately after the initial displacement following the ssc. The broadening of the trace and the increase in the number of lines makes it difficult to resolve the individual lines making up the record.

The ionograms recorded before and after the Doppler recording show quite a marked change as well. Most noticeable is the increase in spread echoes, both in range and frequency, after the Doppler recording, making it impossible to distinguish between ordinary and extraordinary rays at 5 MHz. In addition, a sporadic E trace is visible on the ionogram after the ssc which was not visible before. Further comparison between the two ionograms shows that although h'F is the same on both, the virtual height of the 5MHz reflection level has increased in addition to being spread. Ordinary and extraordinary traces are just visible separately on the ionogram at 12:00 UT and occur at heights of 243 and 233 km respectively. At 12:45 UT, ordinary and extra-ordinary traces cannot be separated, but reflections at 5 MHz occur over the height range 245-315 km, showing an increase in height as the lowest part of the spread is probably associated with the extraordinary ray and the upper part with the ordinary ray reflections.

Understanding the mechanism producing the spreading on the ionograms may lead to an understanding of the Doppler record and in particular may produce a possible explanation for the fine structure observable on the Doppler records.

The rippled contour or corrugated reflector model described in Chapter 4 can be used to explain both spread-F and the unstructured Doppler records. Bowman (1960 a,b) has used the rippled contour model to explain both range and frequency spread as observed on ionograms. Scattering by irregularities

has been suggested by Cornleius et al (1975) as a mechanism for producing the Doppler records at Lyndhurst, Australia. Both scattering from irregularities and reflection from a corrugated reflector can explain unstructured Doppler records and it is necessary to design experiments that uniquely distinguish between the two in order to resolve the ambiguity.

Scattering appears to be the mechanism at times when a Doppler return is received after f_xI has fallen below the Doppler transmission frequency (Cornelius (1975) and Cornelius and Essex (1979a)). No recordings of this type were made at SANAE so that it is not possible to compare the records to detect any differences that there may be between recordings with f_xI above and below the transmission frequency. A further disadvantage of data recorded at SANAE is that no ionograms are available during Doppler recordings as the ionosonde is used for these recordings. This makes it difficult to be sure exactly what changes took place in the ionosphere during recordings. It is therefore difficult to correlate the presence of sporadic E or the occurence of spread-F with simultaneous changes in the Doppler spectrum. The importance of ionograms in simplifying interpretation cannot be stressed enough and it is thus suggested that consideration be given to this aspect when further work is being considered.

Interpretation of the records presented hinges to a large extent on the interpretation of the lines in the record. Two possibilities will be suggested, but it is not possible to distinguish between the two from these records alone. The

first has been mentioned before and is the corrugated reflector model, where the lines are assumed to represent the line of sight velocities of the reflection points on this reflector at any time. The shape of this reflector is changed by the passage of atmospheric waves which distort the iso-ionic contour represented by this reflector. The second possibility is that the lines are produced as a result of reflection or scattering from discrete clouds or volumes of ionization that are essentially free to move independently of each other but may be constrained by the geomagnetic field. During a passage of an atmospheric wave these regions of ionization will experience a vertical force and will move either vertically or along the field line if they are constrained. Movements of these regions will be observed on Doppler records and the lines would represent the line of sight velocities of the individual regions.

These two interpretations would be resolvable if angle of arrival information was available for the Doppler records as the angle at which the largest Doppler shift is received differs in the two cases as a result of the vertical (or near vertical) velocity in one case and horizontal (or near horizontal) velocity in the other.

It must be stressed that these are not the only interpretations that could be made, and that further experimental investigation will reveal the true mechanism behind the Doppler records.

Both these interpretations could be used to explain spread-F on ionograms. It may be possible to compare the results of the two mechanisms suggested with results obtained from the ionograms in order to obtain an indication of the validity of each. It is assumed that range spreading is as a result of different path lengths to reflectors - be they individual regions of ionization or points on an iso-ionic contour. Height changes appearing on the ionogram would be expected to be as a result of the iso-ionic contour moving vertically or as a result of the ionization regions moving vertically. The following analysis of the doppler record was made to check the result obtained from this method. The record was sampled about every 10 seconds and readings were taken of the outer edges of the trace (the individual lines were so close together as to be at the limit of resolution in this case). The individual lines were assumed to represent the line of sight velocities of the reflectors and thus averaging the readings of the outer edges of the trace, at any time, was expected to yield the average line of sight velocity of the reflectors at that time. The curve was then integrated by assuming a constant velocity between the times of samples, calculating the distance travelled in that time and summing the result. This indicated a decrease in height over the recording period (on average). This result is in direct contrast to the ionograms which indicated an increase in virtual height (and thus an increase in phase path) of the 5 MHz level. Figure 5.2 shows a plot of the midpoint of the Doppler spread versus time and Figure 5.3 shows a step by step integration of this curve.

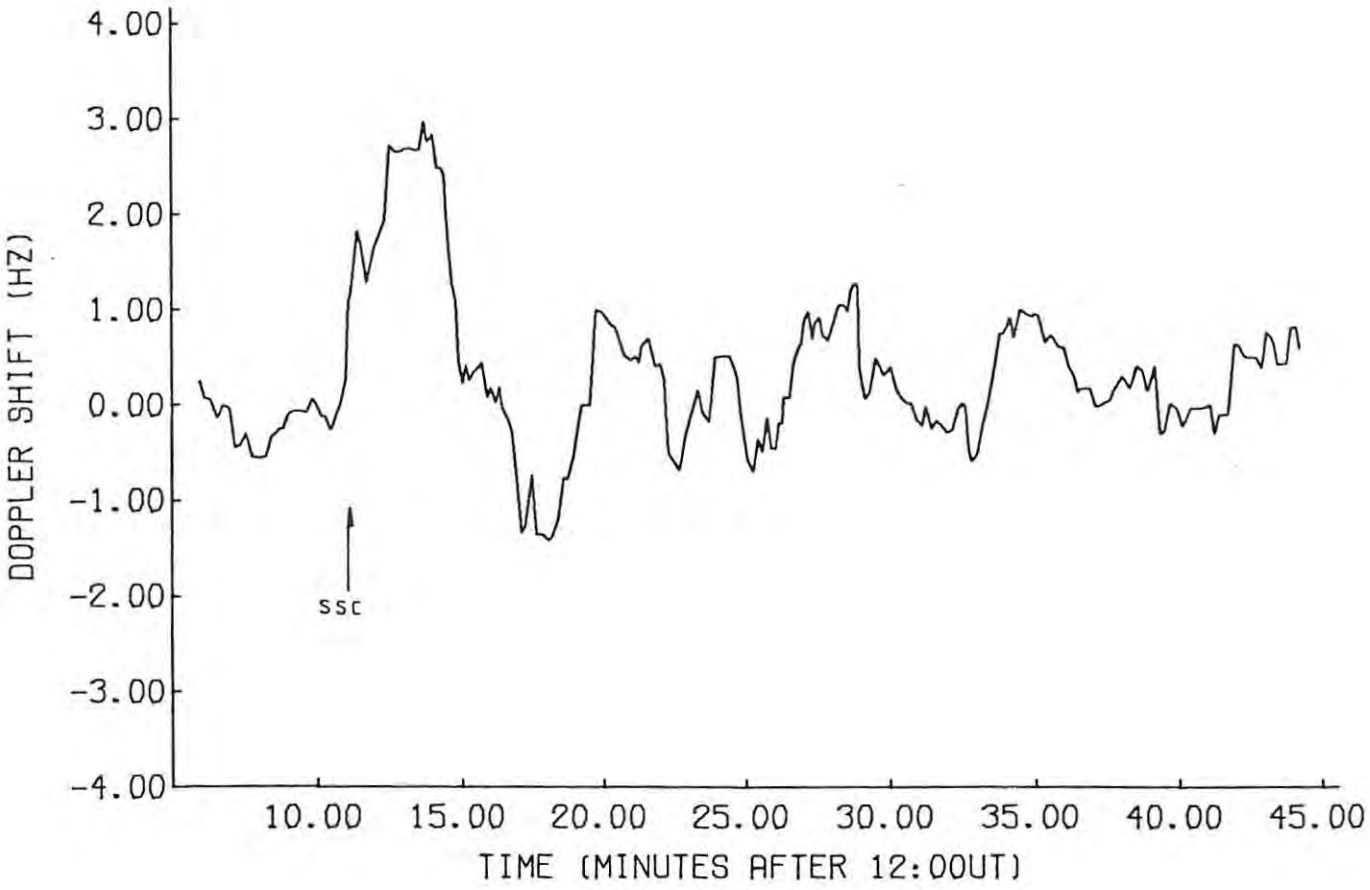

Figure 5,2

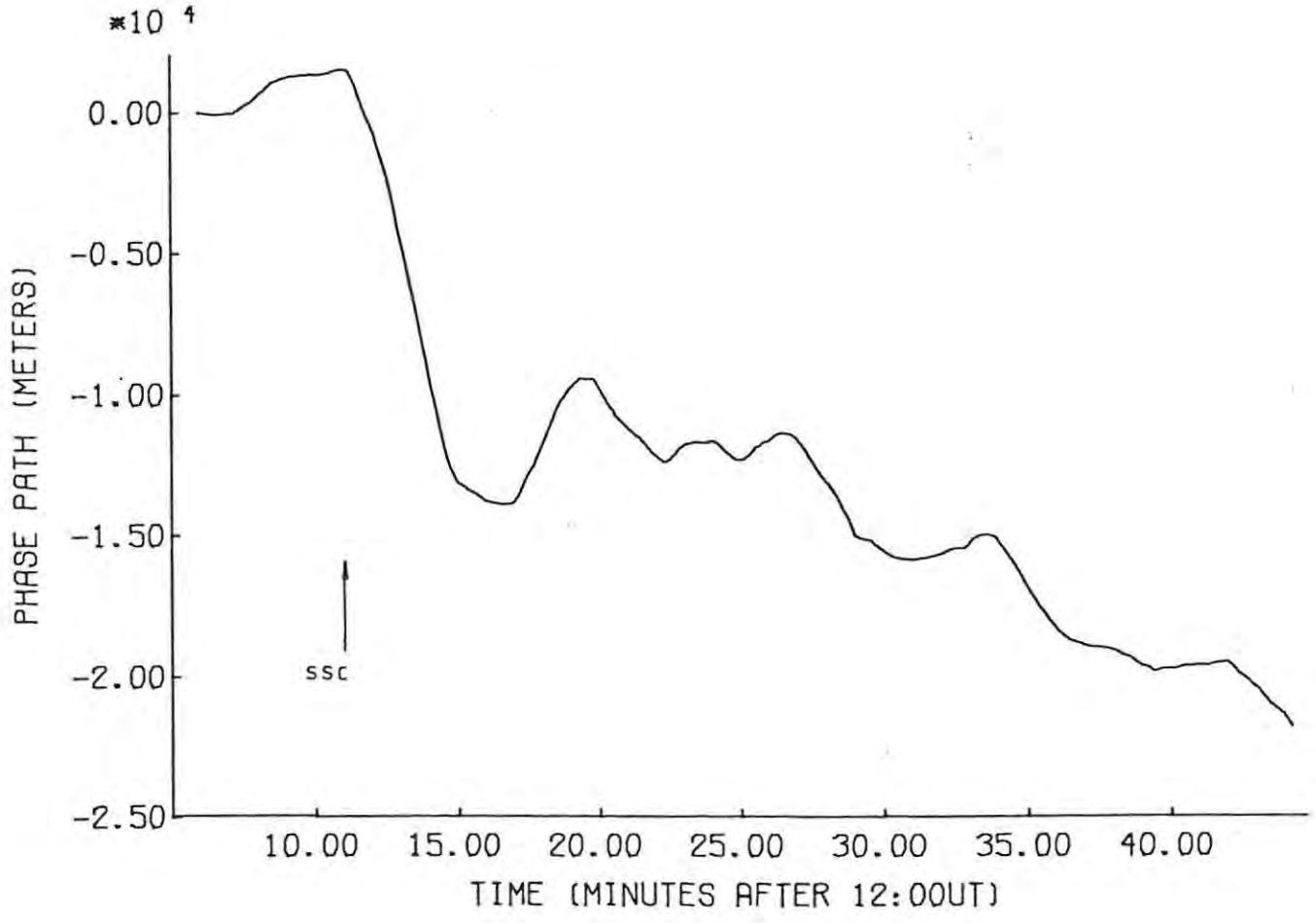

Figure 5,3

The above analysis seems to indicate that the interpretation should be that of a horizontally moving reflector rather than a vertically moving one. With this interpretation, the velocities of the individual reflectors are not related to the Doppler record in the same way. The Doppler components represent the line of sight velocities of the reflection points and thus depend on the horizontal velocity of the contour or volumes of ionization. Movements in a vertical direction will contribute to the Doppler record as well, but it cannot be expected that integration of the mean Doppler curve need bear any relation to the changes in virtual height as detected on the ionograms.

Angle of arrival measurements, together with the Doppler recordings, will help to resolve the interpretation of both the Doppler records and the mechanisms behind the production of "spread-F" on the ionograms. It is hoped that in the near future it will be possible to carry out this type of observation on the chirpsounder in addition to a number of other improvements that are in the constructional stage at present (such as ordinary and extraordinary ray separation).

If a corrugated contour is used as a model of the reflecting surface, it is possible to make some predictions (using results from ionograms) in order to check the validity of the model.

To a first approximation, the difference in virtual height between the upper and lower limits of range spread (at

fixed frequency) can be taken as the difference in virtual range between the vertical and the most off-vertical reflections from the iso-ionic contour under consideration. For this particular case these ranges are 245 km and 315 km respectively. The geometry is shown in Figure 5.4, where the amplitude of the ripple has been greatly exaggerated.

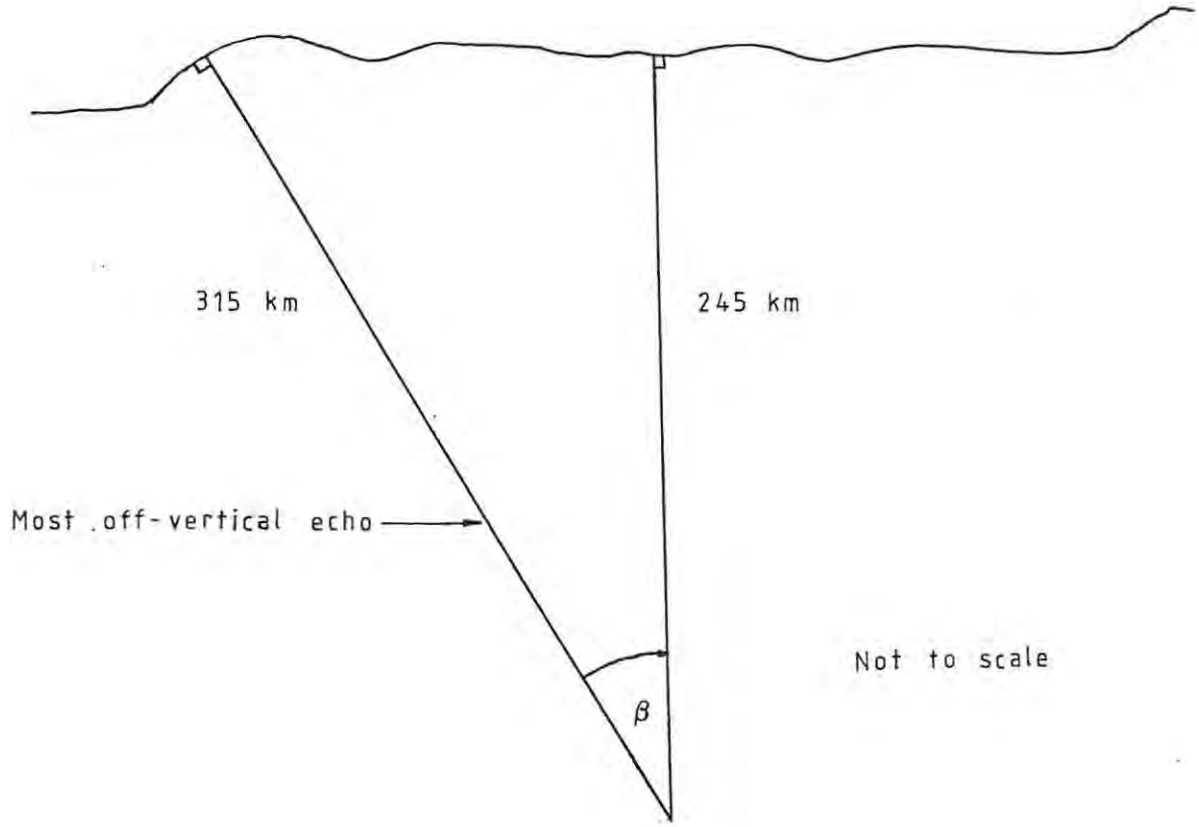

Figure 5.4

Geometry of Model used

The angle of the most oblique echo can be estimated from the geometry of Figure 5.4 and was found to be about 39^0

from the vertical, for this case. In the corrugated reflector model, the highest line of sight velocity occurs at the largest angle (since the contour is moving horizontally). The magnitude of the Doppler shift is proportional to this velocity (equation 4.30) and thus it is reasonable to assume that the outer edges of the Doppler record are as a result of reflections from these oblique echoes. After the sudden commencement, this Doppler frequency was approximately 2Hz. An order of magnitude calculation, using equation 4.30, yields a result of 95 m/s for the horizontal velocity of the reflector. This velocity is of the same order of magnitude as that assumed by Bowman (1960b) in calculations to determine the range spread on ionograms and is certainly within the range of velocities (that have been observed by other techniques) usually associated with atmospheric waves.

Although the interpretation of the Doppler records cannot be conclusive without further investigation and additional information, it is possible to look at the records and derive some useful information from them that can be of benefit in further studies. The parameter that is interesting to observe on the sudden commencement record is the spread of the Doppler trace, as indicated in Figure 5.5.

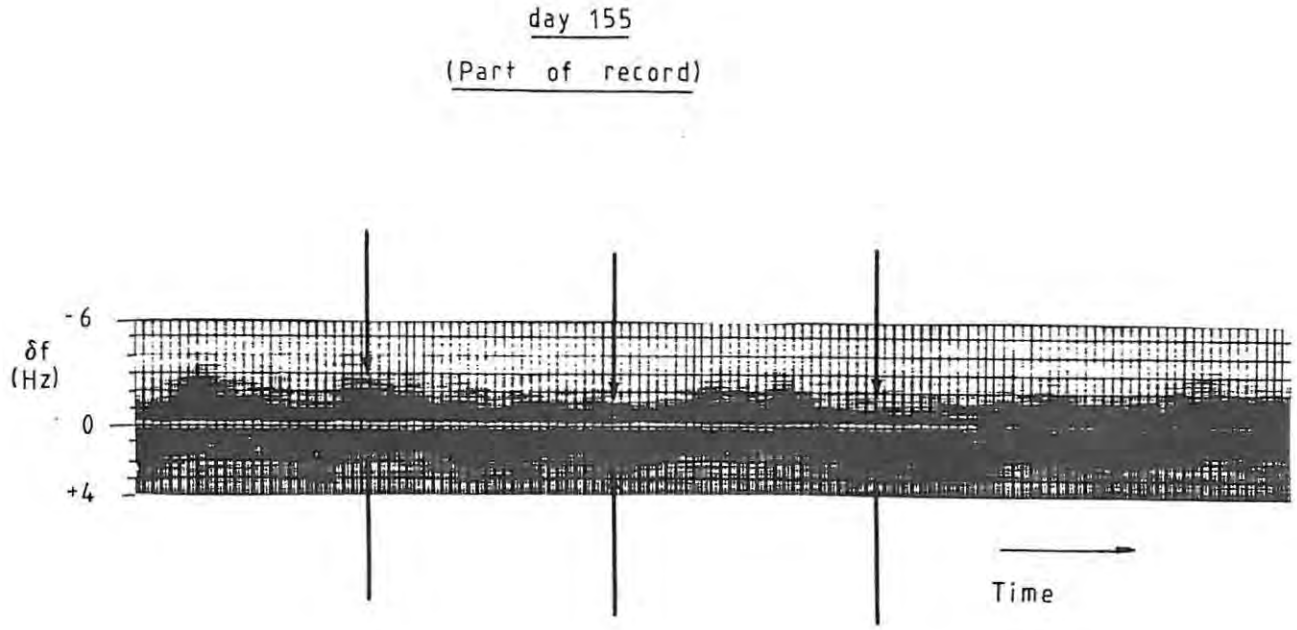

Figure 5.5

Spread on Doppler Record

This spread does not vary very much before the sudden commencement and averages 1.5 - 2.0 Hz in width. After the SCF there is a noticable increase in the width and the average is 3.0 - 3.5 Hz, showing almost a doubling as a result of the ssc. Figure 5.6 shows a plot of the spread versus time. Five-point running averages have been taken in order to remove the high frequency fluctuations of the curve that were introduced when the spread was measured.

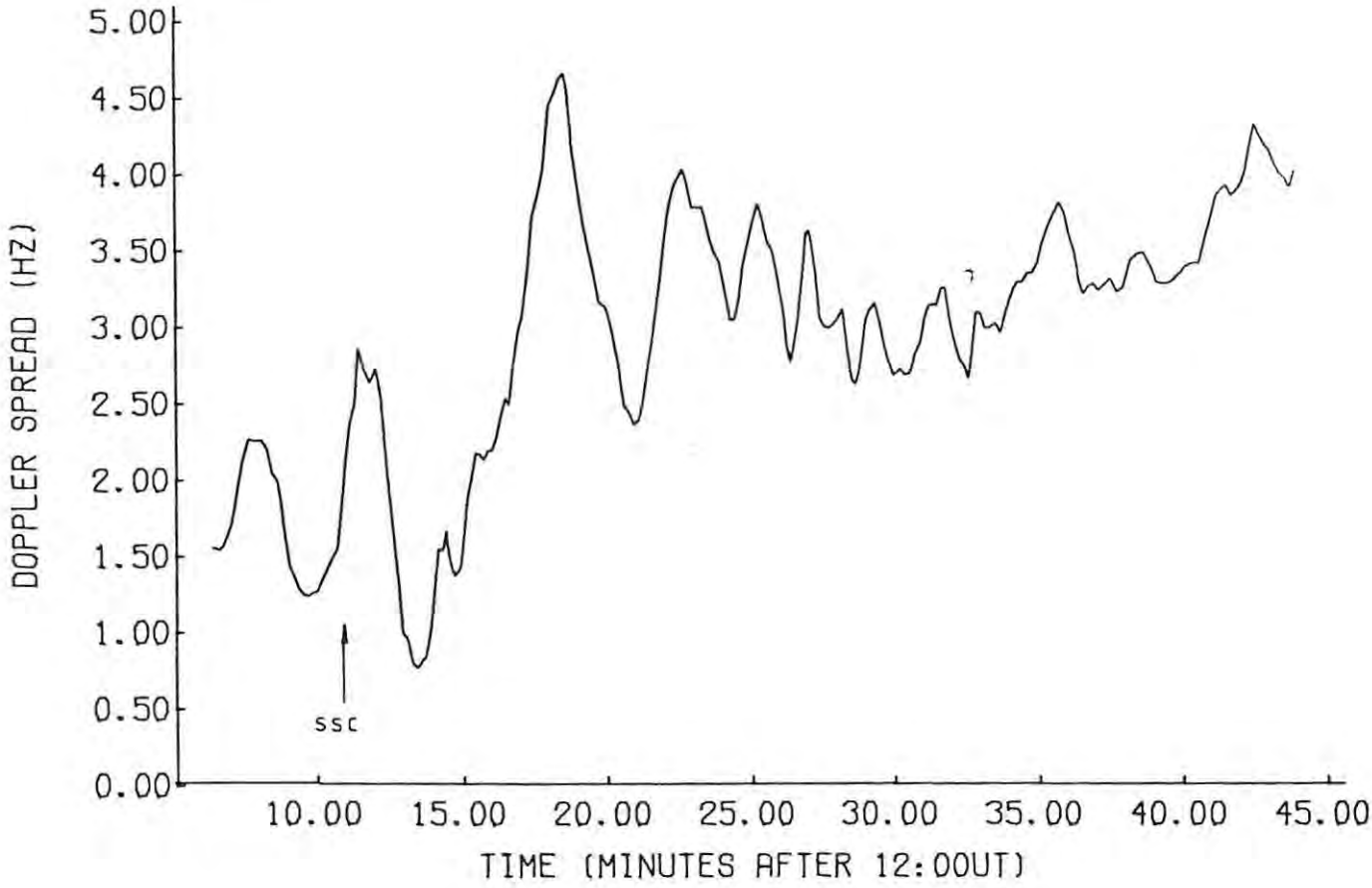

Figure 5.6

This increase in the spread of the spectrum could occur as a result of increased tilts (larger amplitude to wavelength

ratio) or increased velocity of the corrugated reflector, if that interpretation is used. It is not unreasonable to expect that a sudden commencement would produce a change in the atmospheric waves travelling at ionospheric heights or a change in the "patchiness" of the ionosphere, both of which could be detected as increased spread on Doppler records.

It is important to remember that only a single ssc has been recorded using the Chirpsounder Doppler system and it is therefore not possible to draw definite conclusions. It will suffice to say that the record under consideration is interesting and does show some features that are worth investigating in greater detail in order to understand more fully the mechanisms behind spread-F, atmospheric waves and magnetic sudden commencements. Additional data would be useful in confirming which features of the present record are characteristic of the phenomenon under investigation.

5.3 Solar Flare - 14th August, 1978 (day 226)

A H_α solar flare was reported in Solar-Geophysical Data, Prompt reports to have occurred during one of the Doppler recording periods. The start time was given as 11:52 UT on day 226 (1978) and its effect could be observed on the Doppler record even though the Doppler recording ended at 11:58 UT (before the maximum of the flare at 12:48). The flare was classified to be of importance SN and type C.

General features of the Doppler record are similar to the record discussed above but the individual lines making up the record are resolvable in this case until about the time of the flare when the resolution becomes less distinct. Analysis of the record was carried out in a similar fashion to that of the sudden commencement record, but samples were taken every 20 seconds and individual frequencies of the lines were measured before averaging these readings at any one time. A plot of the mean line of sight velocities (as determined in this way) is shown in Figure 5.7. Integration of this curve produced the curve shown in Figure 5.8.

The effect of the flare is only just noticable on the curve of mean Doppler velocities; the mean Doppler shift becomes more negative for a short period after the H_α flare. The integral of this curve shows this quite clearly as an increase in the phase path during this time. The nett change in phase path over the recording period was just less than 1.5 km.

The ionograms recorded at 11:30 and 12:00 UT show a slight increase in virtual height of the 5 MHz level. The value of $f_o F_2$ remained almost unchanged but there was an increase in spread-F at 12:00 UT. An oblique "satellite trace" was present at 5 MHz together with a second order reflection on both ionograms. The ionograms are reproduced in Figure 5.9.

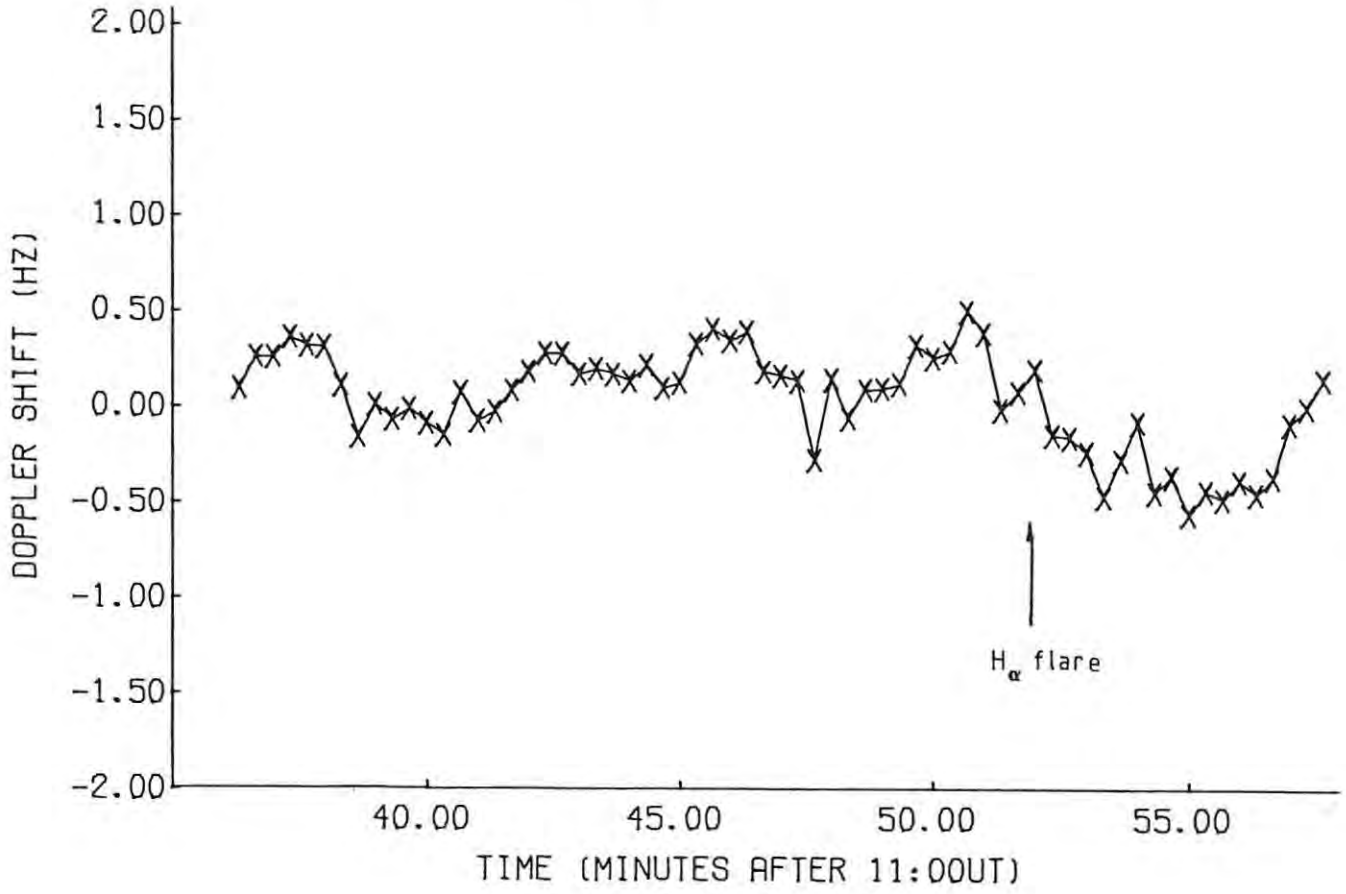

Figure 5,7

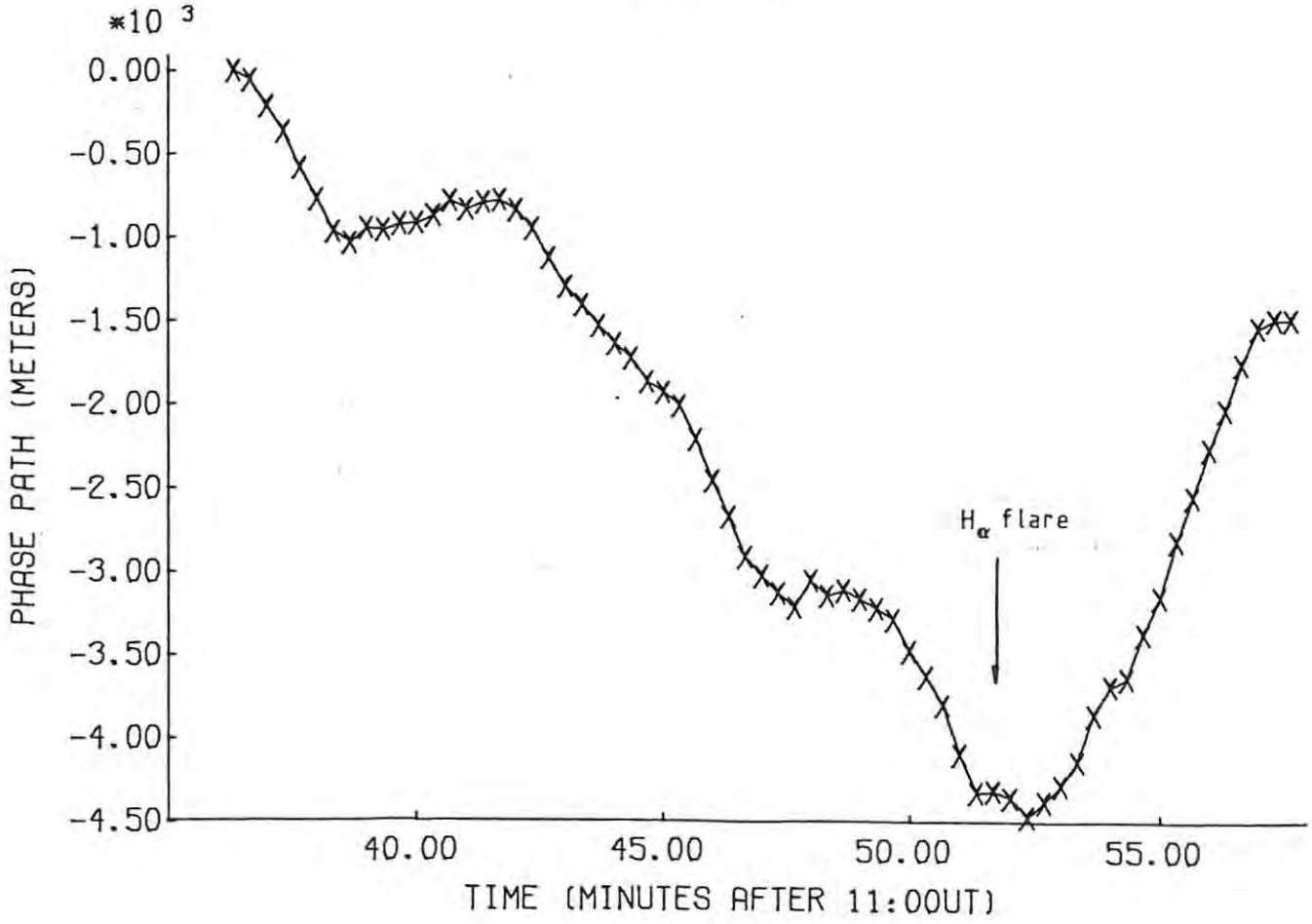

Figure 5,8

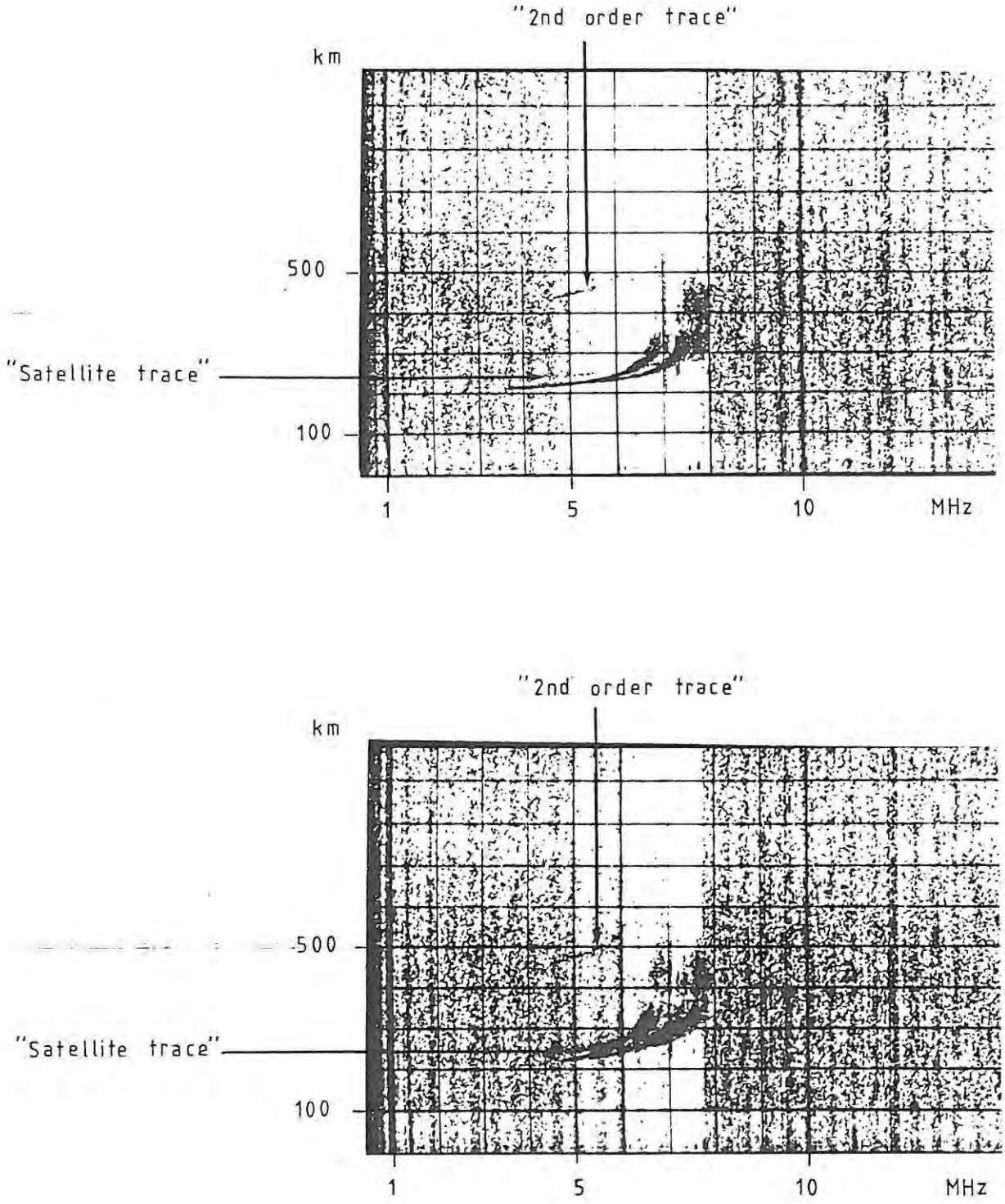
"2nd order trace"
km
500
"Satellite trace"
100
1
5
10
MHz
"2nd order trace"
km
500
"Satellite trace"
100
1
5
10
MHz

Figure 5,9

Lack of ionograms during the recording made interpretation slightly more difficult, once again, but it is reasonable to assume that there was no range spread at 5 MHz throughout the recording period. As before, the Doppler spread present on the record was interesting to observe and is plotted against time in Figure 5.10.

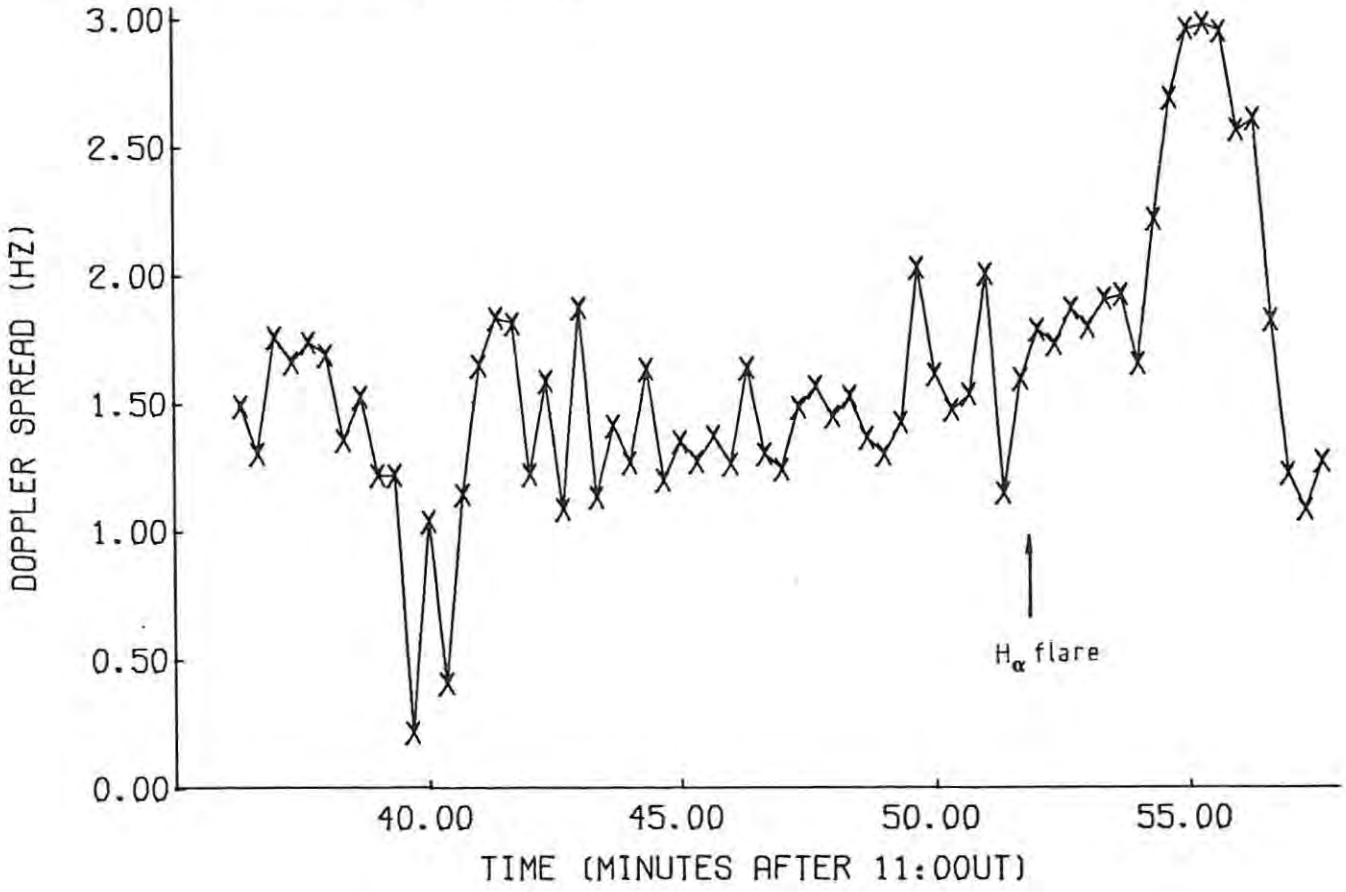

Figure 5.10

This curve shows that the spread was of the order of 1.5 - 2.0 Hz wide for most of the recording period. The sudden decrease near to 11:40 was caused by an alteration of the gain setting for a short period. More interesting is the sudden increase soon after the time of the solar flare. The 1.5 - 2.0 Hz spread before the flare agrees well with the spread present

before the sudden commencement event discussed earlier in this chapter. This could be taken to be the "normal" or "quiet" spread and does not appear as range spread on the ionograms. A corrugated reflector has been suggested as the mechanism behind the spreading observed during the sudden commencement, and can be used to explain this spreading as well. The resolution on the ionograms may not be sufficient to show range spreading when Doppler records show spread that is of the order of 2.0 Hz wide.

There is another possibility that should, however, be considered. Changes of the phase refractive index, μ, along the ray path can contribute to the Doppler shift as was shown in Chapter 4 (equation 4.26). Thus, movements of clouds or layers of ionization below the level of reflection may contribute to the Doppler shift. It is possible that these clouds have a plasma frequency that is below the minimum frequency observed on the ionogram and in such cases it will be difficult to detect their presence by means of ionograms. Movements of clouds below the level of reflection could be used in conjunction with a corrugated reflector model in explaining broad Doppler records or they could be used with a smooth reflecting layer without tilts.

Determining which of many mechanisms are responsible for broad-unstructured Doppler records is a difficult task and work designed to distinguish between the different

possibilities is essential. Mention was made in Chapter 4 that ionization in E - F_1 regions was thought to be the cause of solar-flare effects on Doppler records rather than variations in the height of reflection (according to the literature). There is some evidence of this in this case as well. N-h profiles produced from the ionograms recorded at 11:30 and 12:00 UT show that the shape of the upper-ionosphere remained very nearly identical in both cases, the only difference was the starting height of the profile. The starting height is determined from the first point on the ionogram and the profile is calculated from this point onwards. This implies that if the starting heights were equal, the profiles would be the same. Changes in ionization below f_{min} are not observable on the ionogram except as a retardation of the signal which would result in an increase in virtual height, the increase becoming less with increasing frequency. Thus increased ionization, in lower ionospheric regions and with plasma frequency less than f_{min}, could account for the increased height observed on the N-h profile and is a more attractive proposition than bulk motion of the ionosphere with the shape unchanged.

The degree to which ionization movements were responsible for the Doppler record, and in particular the part of the record associated with the flare, is uncertain and it is not possible to interpret the records conclusively. The full effect of the flare very likely appeared after Doppler recording

ceased but there is still evidence of its effect on the record during the early stage. There is certainly a lot of scope for experimentation with particular emphasis on distinguishing between movements of reflection height and movements of ionization below the level of reflection. Work aimed at resolving some of the ambiquities in interpretation would also be very helpful in understanding the mechanisms behind the movements that are detected.

The use of more than one sounding frequency makes it possible to be more certain about the type of movement occuring (Namazov et al (1976)) and it is suggested as an improvement to the present system used on the chirpsounder.

5.4 General Discussion

Some of the common features of the chirpsounder Doppler records will be discussed and these records will be compared with other records as shown in the literature. Suggestions will be made as to the reasons for some of the differences.

Most noticeable on every record produced using the chirpsounder at SANAE were the lines or fine structure resolvable in the rather broad trace. Some suggestions have

been put forward to explain the occurence of the lines as well as the broad nature of the trace. The lengths of the lines tend to be fairly similar but there are occasions when fairly long continuous lines have been present. The average length of lines suggests that reflections producing the individual lines persist for something of the order of 40 seconds to a minute.

On one occasion a trace of fairly constant slope was observed to extend from the broad trace. Similar traces were observed in experiments conducted during aircraft flights in the northern polar region by Basler et al (1973) and were interpreted as produced by reflections from moving irregularities. The Chirpsounder record on that day is shown in Figure 5.11 and has a certain amount of symmetry. The spread is of the order of 1.5 - 2.0 Hz wide (except during the movement of the irregularity) and is fairly symmetrically placed about the zero line. Regions of strong intensity appear to have similar regions reflected about the zero line. The trace extending from the broad trace is also seen to have a symmetrical trace although very much weaker. Reasons for the symmetry are not known. This record was analysed in the same way as the solar flare record was - individual frequencies sampled every 20 seconds and the average Doppler frequency determined at each of these times. The results are plotted in Figure 5.12 and the integral of this curve in Figure 5.13.

16th August, 1978

(day 228)

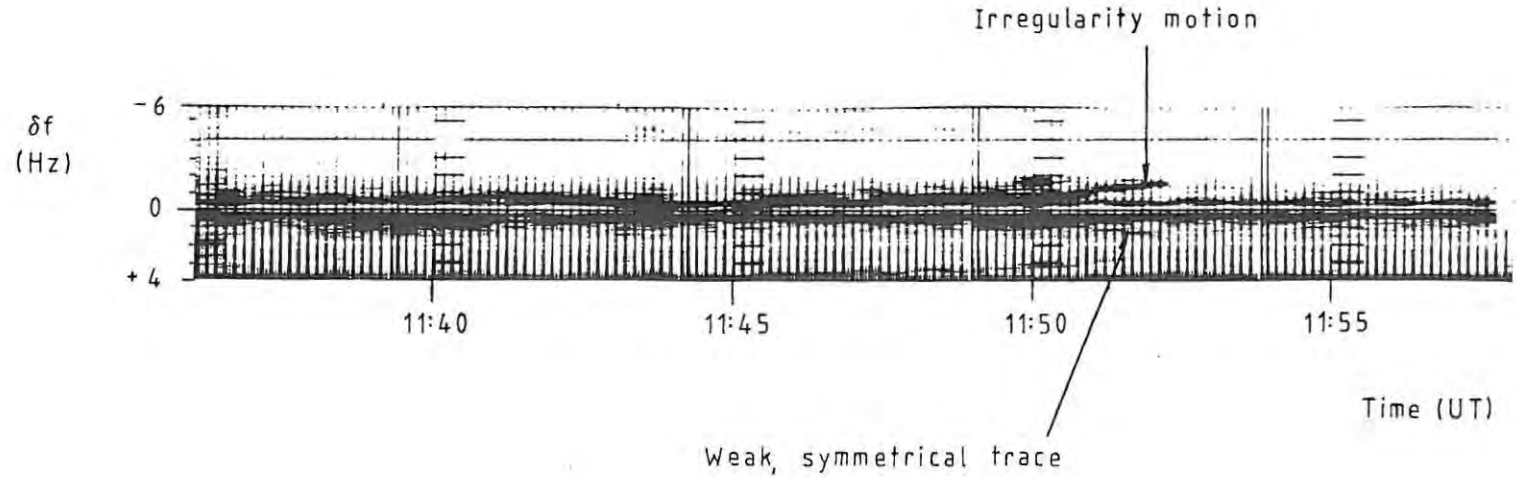

Figure 5.11

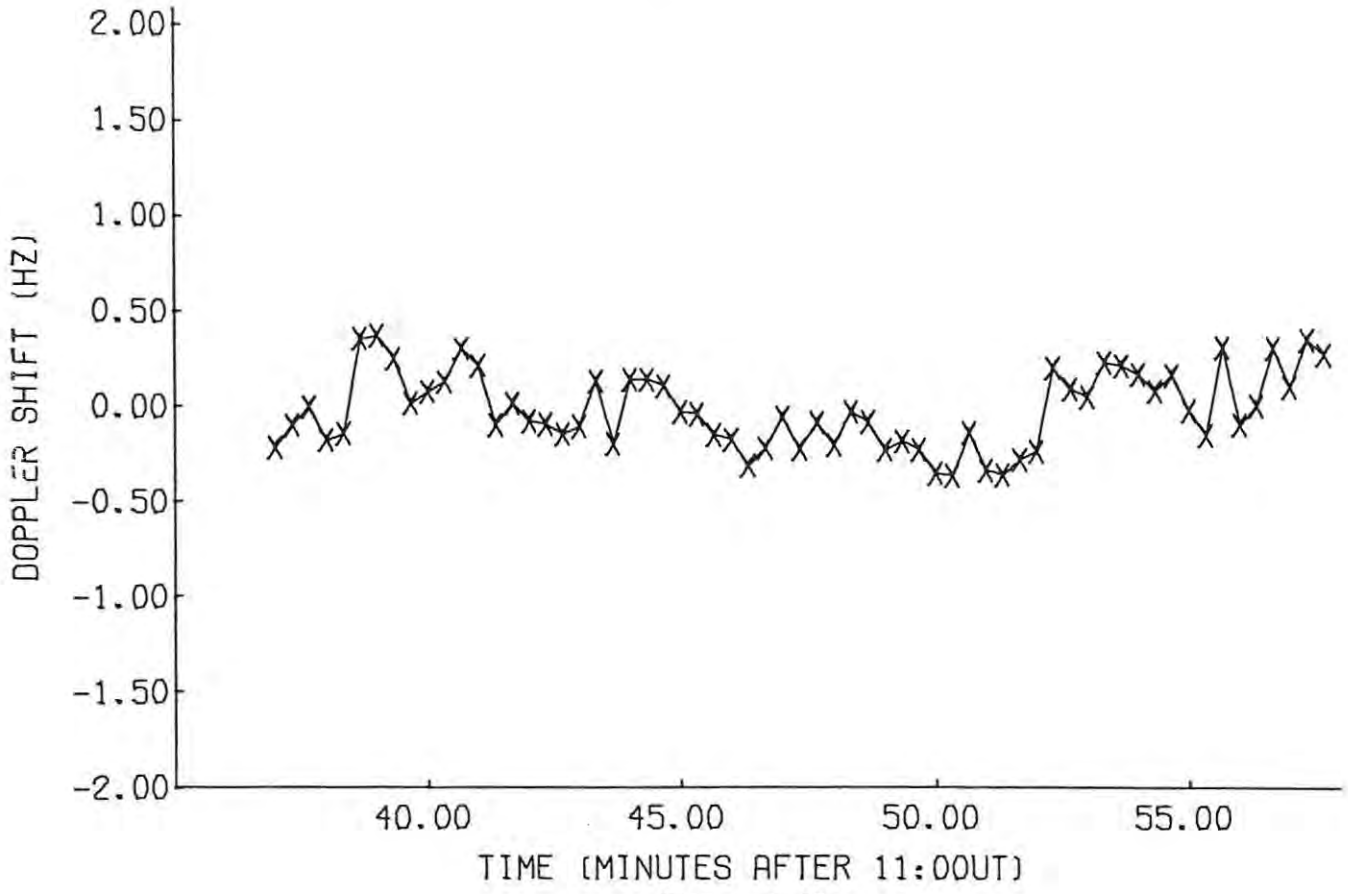

Figure 5,12

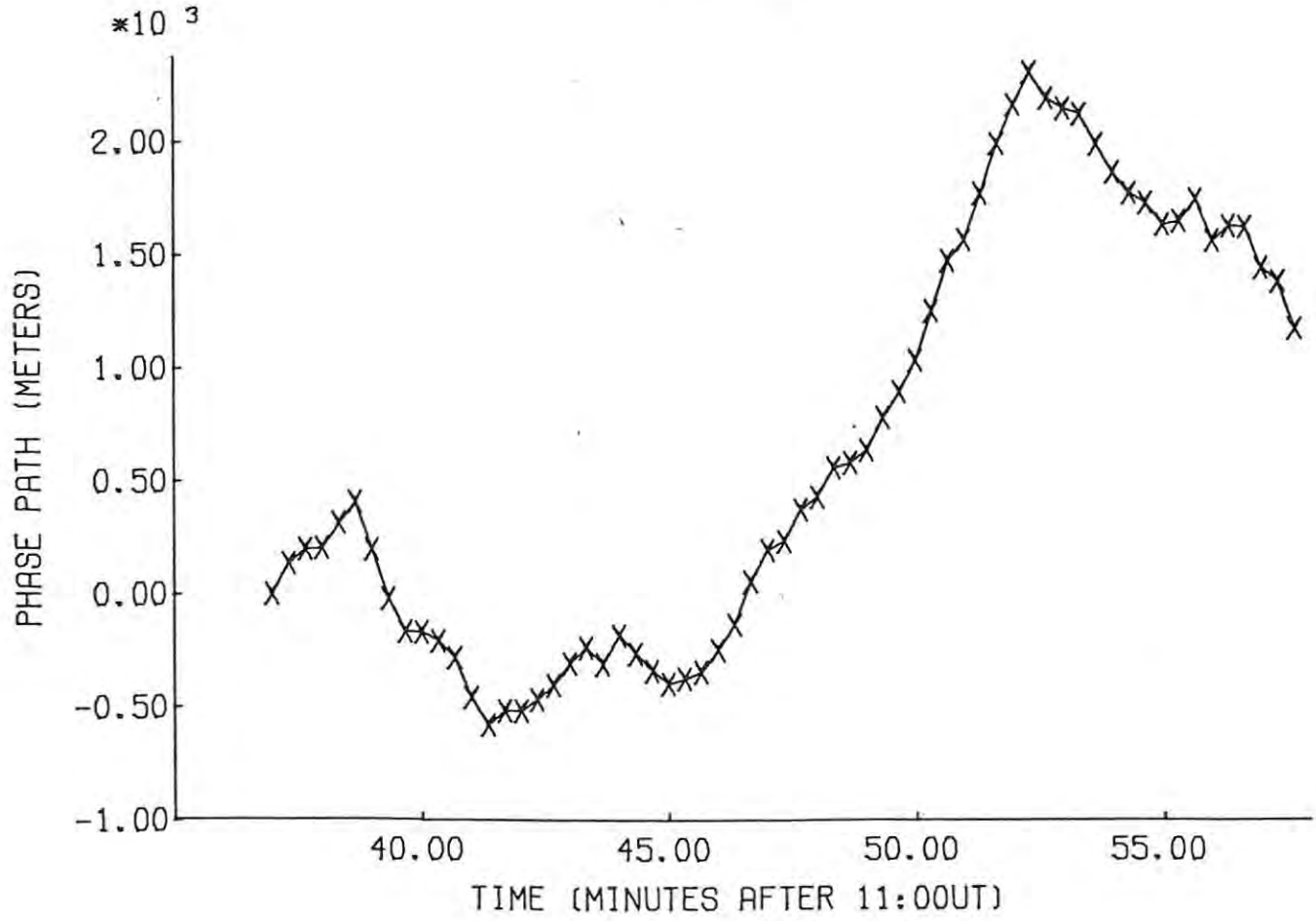

Figure 5,13

Figure 5.13 suggests that there may have been a wavelike disturbance passing overhead during the recording.

The remainder of the Doppler records do not show any special features but are consistent with the general features of the records already discussed. Attempts were made to correlate spread-F on the ionograms with features of the records but range spread at 5 MHz was not present on any of the ionograms immediately before or after Doppler recordings. Slightly more success was obtained with sporadic E checks when one occasion was found with f_oE_s above 5 MHz before the recording and below 5 MHz after the recording. The Doppler record shows a distinct change in character at one time but it is not possible to be certain that this change is associated with f_oE_s translations through 5 MHz, but this is likely. Similar changes in the nature of the Doppler record were noted by Cornlius et al (1975) when f_oE_s moved across the Doppler sounding frequency. Lack of ionograms during the recording is the reason for the uncertainty in the interpretation of the SANAE record of day 348 (1978), shown in Figure 3.8 (Chapter 3).

Comparison of the chirpsounder Doppler records with those appearing in the literature from time to time is often made difficult when records extending over several hours are shown and are often not very much more than 10 cm long. It does appear that most records do not have the resolution shown by the chirpsounder records, if one is to judge by the resolutions quoted in the papers. Most Doppler records noted in the literature

are made up of a well defined trace (often fairly broad in character). Variations in this trace are often observed and deviations associated with flares, ssc's and so on have been discussed earlier. Some records do show evidence of fine structure (for example Cornelius et al (1975), Cornelius and Essex (1979 a,b)). Fine structure has also been observed by Dudeney (1979, private communication) by using a different technique for displaying previously well defined traces. Fine structure may thus be a feature of most Doppler records and the displaying technique may be responsible for it not being observed and studied earlier.

It is possible that the fine structure is a feature unique to the polar regions (Dudeney's records were from Argentine Island) and if this is so, it is in need of explanation.

It is believed that the fine structure of the chirpsounder records is the most important aspect of the data and that a lot more attention should be given to the understanding of these details.

CHAPTER 6

CONCLUSION

The experimental investigations undertaken at SANAE using the chirpsounder have shown that it is indeed possible to use this equipment as an H.F. Doppler sounder and that data recorded show some very interesting features not often discussed in the literature.

In particular, the fine structure observable on the records is interesting and investigation of the mechanism producing this is needed. The long integration time used on the spectrum analyser as well as the "overlapping window" technique is suggested as the reason that fine structure has been observed with this Doppler system, while little mention has been made of it in the literature. There is some evidence that this structure is a feature of high-latitude stations rather than a general feature, but this too must be confirmed by further experimentation.

When further experimentation is considered, emphasis should be placed on eliminating rival possibilities, and experiments designed to do this will be of the greatest benefit in leading to an understanding.

For the chirpsounder system, there are some developments currently taking place that will be of use when this Doppler system is used for further work. The major advance will be the availability of digital data stored on paper tape in addition to the analogue data on photographic film. This system is due to be installed in the chirpsounder at SANAE in 1980 and will be followed by further improvements when the microprocessor unit is installed to replace Logchirp control as the controlling unit of the chirpsounder. These improvements will not only allow greater flexibility in any Doppler experiments conducted, such as choice of sounding and offset frequencies, but will allow separation of ordinary and extra-ordinary rays together with angle of arrival measurements during the Doppler recordings (Evans (1979), private communication). An alternate method of separating O and X rays has been suggested by Burnside and Gaede (1979), in addition to having ionograms during the Doppler experiments.

The conversion of the chirpsounder to allow digital output (ionograms as well as doppler) is effected by the installation of a hardware Fast Fourier Transform (FFT) unit designed and built by Fisher (1979). This will allow data analysis of Doppler records to be carried out in a more flexible and accurate way. Data produced by this unit can later be transformed back into the time domain and thus will allow the integration time to be varied as well as analysis in this

domain. This has been one of the major drawbacks of having data recorded on film where the phase information in the frequency domain has been completely lost and amplitude information is difficult to determine with any certainty.

There are a number of minor improvements that will be part of the introduction of the microprocessor control and in particular, ionograms interspersed with Doppler recording as well as automatic time marks during Doppler recordings will be useful. Software selection of recording mode (vertical, oblique or Doppler) will have the advantage of reducing operator attendance during Doppler recordings as this selection will be made in advance.

It is hoped that the improvements mentioned above will make the Chirpsounder an even more powerful Doppler sounder than it is at present, even though it is primarily an ionosonde, and that Doppler experiments will be continued with this equipment and the techniques improved.

Not much attempt has been made to produce answers to the many questions that have been raised by these ionospheric Doppler studies. In fact, more questions have been raised and left unanswered. If this thesis suggests experiments that may be aimed at answering these questions, then I have succeeded in my immediate goal.

REFERENCES

Afraimovich E.L., Vugmeister G.O., Zakharov V.N., Kalikhman A.D. and Korolev V.A. :
Experimental Investigation of Doppler Frequency and Angle Fluctuations of Radio Signal Arrival at Vertical Sounding of the F_2 Ionosphere Region. (in Russian) English Translation in Radio Phys. and Quantum Electron. (USA, 1976)

Akasofu S. -I. and Chapman S. :
The Sudden Commencement of Geomagnetic Storms. IAGA Bulletin No. 16C, Rapid Magnetic Variations (Utrecht Symposium, 1959)

Andrews M.K., Thomson N.R. :
Doppler Shifts on Whistler Mode Signals Received at Siple Station Antarctica.
Geophys. Res. Lett. 4 (1977) 399-401

Baker D.C. and Gledhill J.A. :
An Unusual Travelling Disturbance in the F-Region of the Ionosphere.
J. Atmos. and Terr. Phys. 27 (1965) 1223-1227

Baker D.M. and Davies K. :
Waves in the Ionosphere Produced by Nuclear Explosions.
J. Geophys. Res. 73 (1968) 448-451

Basler R.P., Scott T.D. and Dupuy P.L. :
Irregularity Motions in the Polar Ionosphere.
Radio Sci. 8 (1973) 745-751

Bennett J.A. :
The Calculations of Doppler Shifts due to a changing Ionosphere.
J. Atmos. and Terr. Phys. 29 (1967a) 887-891

Bennet J.A. :
The Relation Between Group and Phase Path.
J. Atmos. and Terr. Phys. 29 (1967b) 893-896

Bennet J.A. :
The Ray Theory of Doppler Frequency Shifts.
Aust. J. Phys. 21 (1968) 259-272

Blagoveshchenskaya N.F., Blagoveshchenskaya D.V., Kurchenko Yu.A.:
Experimental Investigation of HF Signal Fluctuation Spectra in the Auroral Zone II Effect of Geophysical Conditions on Spectral Statistics.
Geomag. And Aeron. 16 (1976) 166-167

Bowman G.G. :
Further Studies of "Spread-F" at Brisbane.
I Experimental Planet Space Sci. 2 (1960a) 133-149

Bowman G.G. :
Further Studies of "Spread-F" at Brisbane.
II Interpretation Plant Space Sci. 2 (1969b) 150-156

Bowman G.G. :
Movements of Ionospheric Irregularities and Gravity Waves.
J. Atmos. and Terr. Phys. 30 (1968) 721-734

Burnside R.G. and Gaede H. :
Measurements of O and E Mode Ionospheric Doppler Shifts with a Rotating Antenna.
S. Afr. J. Phys. 2 (1979) 93-97

Chan K.L. and Villard O.G. Jr :
Observation of Large-scale Travelling Ionospheric Disturbances by Spaced-path High Frequency Instantaneous Frequency Measurements.
J. Geophys. Res. 67 (1962a) 973-988

Chan K.L., Kanellakos D.P. and Villard O.G. Jr :
Correlation of Short Period Fluctuations of the Earth's Magnetic Field and Instantaneous Frequency Measurements.
J. Geophys. Res. 67 (1962b) 2066-2072

Chan K.L. and Villard O.G. Jr :
Sudden Frequency Deviations Induced by Solar Flares.
J. Geophys. Res. 68 (1963) 3197-

Chapman S. and Bartels J :
Geomagnetism. Vol I and II.
Oxford, Clarendon Press (1940)

Cornelius D.W., Joyner K.H., Dyson P.L. and Butcher E.C. :
Scattering from F-Region Irregularities at 4.5 and 7.5MHz.
J. Atmos. and Terr. Phys. 37 (1975) 769-776

Cornelius D.W. and Essex E.A. :
HF Doppler Observations of 23 October, 1976
Total Solar Eclipse over South Eastern Australia.
J. Atmos. and Terr. Phys. 40 (1978) 497-502

Cornelius D.W. and Essex E.A. :
HF Doppler Observations Associated with Spread-F.
J. Geophys. Res. 84 (1979a) 1361-1368

Cornelius D.W. and Essex E.A. :
Observations of Mid-latitude Sporadic E using the
HF Doppler Technique.
J. Atmos. and Terr. Phys. 41 (1979b) 481-499

Czechowsky P. :
Doppler Shift of Auroral Backscatter Signals.
J. Geophys. Res. 40 (1974) 229-237

Davies K. and Baker D.M. :
On Frequency Variations of Ionospherically Propagated
HF Radio Signals.
Radio Sci. 1 (1966) 545-556

Davies K. and Donnelly R.F. :
An Ionospheric Phenomenon Associated with Explosive
Solar Flares.
J. Geophys. Res. 71 (1966) 2843-2845

Davies K., Watts J.M. and Zacharisen D.H. :
A Study of F_2- layer effects as Observed with a Doppler
Technique.
J. Geophys. Res. 67 (1962) 601-609

De Mendonca F. :
Ionospheric Electron Content and Variations Measured by Doppler Shifts in Satellite Transmissions.
J. Geophys. Res. 67 (1962) 2315-

De Mendonca F. and Garriott O.K. :
The Effect of the Earth's Magnetic Field on Measurements of the Doppler Shift of Satellite Radio Transmissions.
J. Geophys. Res. 67 (1962) 2062-

Doupnik J.R. and Nisbet J.S. :
Fluctuations of Electron Density in the Daytime F-region.
J. Atmos, and Terr. Phys. 30 (1968) 931-962

Dudeney J.R. and Jones T.B. :
Doppler Radio Soundings of the Ionosphere over the Antarctic Peninsula.
Antarctic J. XI (1976) 102-

Dudeney J.R., Jones I.B., Kressman R.I. and Spracklen C.T. :
Radio Wave Doppler Studies of the Antarctic Ionosphere.
Phil. Trans. R. Soc. Lond. B 279 (1977) 239-246

Dudeney J.R. :
Private Communication (1979).

Duffus H.J. and Boyd G.M. :
The Association between ULF Geomagnetic Fluctuations and Doppler Ionospheric Observations.
J. Atmos. and Terr. Phys. 30 (1968) 481-496

Dyson P.L. :
Relationships between the Rate of Change of Phase Path (Doppler Shift) and Angle of Arrival.
J. Atmos . and Terr. Phys. 37 (1975) 1151-1154

Essex E.A. :
Comparison of Ionospheric Gravity Wave Periods as Measured by Different Experimental Techniques.
J. Atmos. and Terr. Phys. 37 (1975) 1349-1356

Essex E.A. and Hibberd :
Frequency and Spatial Correlations of Fading Radio Echoes from the Ionosphere.
J. Atmos. and Terr. Phys. 30 (1968) 1019-1032

Evans G.P. :
Private Communication Re microprocessor Control of Chirpsounder.
Rhodes University (1979)

Fisher J.S. :
A Real Time Fast Fourier Transform Analyser.
M.Sc. Thesis submitted to Rhodes University (December 1979)

Fox C. :
Calculus of variations.
Oxford University Press (1963)

Fooks G.F. :
Ionospheric Irregularities and the Phase Paths of Radio Waves.
J. Atmos. and Terr. Phys. 24 (1962) 937-947

Francis S.H. :
A Theory of Medium-scale Travelling Ionospheric Disturbances.
J. Geophys. Res. 79 (1974) 5245-5260

Gautier T.N. :
Generality of the Relation between the Group and the Phase Path.
J. Atmos. and Terr. Phys. 28 (1966) 1125-1128

Georges T.M. :
HF Doppler Studies of Travelling Ionospheric Disturbances.
J. Atmos. and Terr. Phys. 30 (1968) 735-746

Haldoupis C., Koehler J.A. and Sulko G.J. :
A VHF Bistatic Doppler System for Radio Investigations of the Auroral Ionosphere.
J. Phys. E. 11 (1978) 135-138

Hines C.O. :
Some Consequences of Gravity-wave Critical Layers in the Upper Atmosphere.
J. Atmos. and Terr. Phys. 30 (1968a) 837-844

Hines C.O. :
An Effect of Molecular Dissipation in Upper Atmospheric Gravity Waves.
J. Atmos. and Terr. Phys. 30 (1968b) 845-850

Hines C.O. :
An Effect of Ohmic Losses in Upper Atmospheric Gravity Waves.
J. Atmos. and Terr. Phys. 30 (1968c) 851-856

Hooke W.H. :
Ionospheric Irregularities Produced by Internal Atmospheric Gravity Waves.
J. Atmos. and Terr. Phys. 30 (1968) 795-823

Huang Y-N., Najitja K. and Yuen P. :
The Ionospheric Effects of Geomagnetic Sudden Commencements as Measured with an HF Doppler Sounder at Hawaii.
J. Atmos. and Terr. Phys. 35 (1973) 173-181

Huang Y-N. :
Modelling HF Doppler Effects of Geomagnetic Sudden Commencements.
J. Geophys. Res. 81 (1976) 175-182

Ichinose T. and Ogawa T. :
HF Doppler Observation Associated with Magnetic Storm.
J. Atmos. and Terr. Phys. 36 (1974) 2047-2053

Ichinose T. and Ogawa T. :
Internal Gravity Waves Deduced from the HF Doppler Data During the April, 19, 1958 Solar Eclipse.
J. Geophys. Res. 81 (1976) 2401-2404

Jacobs J.A. and Watanabe T. :
Doppler Frequency Changes in Radio Waves Propagating Through a Moving Ionosphere.
Radio Sci. 3 (1966) 257-264

Kanellakos D.P., Chan K.L. and Villard O.G. Jr :
On the Altitude at which Solar-Flare-Induced Ionization is Released.
J. Geophys. Res. 67 (1962) 1795-1804

Kanellakos D.P. and Villard O.G. Jr :
Ionospheric Disturbances Associated with the Solar Flare of September 28, 1961.
J. Geophys. Res. 67 (1962) 2265-2278

Kato S. and Matsushita S. :
Space Charge Waves and Ionospheric Irregularities.
J. Atmos. and Terr. Phys. 30 (1968) 857-

Kern J.W. :
A Note on the Generation of the Main-phase Ring Current of a Geomagnetic Storm.
J. Geophys. Res. 67 (1962) 3737-3751

Kelso J.M. :
Doppler Shifts and Faraday Rotation of Radio Signals in a Time Varying, Inhomogeneous Ionosphere. Part I Single Signal Case.
J. Geophys. Res. 65 (1960) 3909-3914

Kelso J.M. :
Doppler Shifts and Faraday Rotation of Radio Signals in a Time Varying, Inhomogeneous Ionosphere. Part II Two-signal Case.
J. Geophys. Res. 66 (1961) 1107-1115

Kent G.S. and Wright R.W.H. :
Movements of Ionospheric Irregularities and Atmospheric Winds.
J. Atmos. and Terr. Phys. 30 (1968) 657-691

Kimura I. and Nishina R. :
Doppler Shift in an Inhomogeneous Anisotropic Medium.
Rep. on Iono. and Space Res. in Japan 21 (1967) 187-192

Lee J.R. :
Advanced Calculus with Linear Analysis.
Academic Press (1972)

Lee K.S.H. and Papas C.H. :
Doppler Effects in Inhomogeneous Anisotropic Ionized Gases.
J. Math. Phys. 42 (1963) 189-199

Lomax J.B. and Nielson D.L. :
Observation of Acoustic-gravity Wave Effects Showing Geomagnetic Field Dependence.
J. Atmos. and Terr. Phys. 30 (1968) 1033-1050

Lyon G.F. :
HF Doppler Studies of Travelling Ionospheric Disturbances.
Phys. Can. 29 (1973) 23

Lyon G.F. :
The Corrugated Reflector Model for One-hop Oblique Propagation.
J. Atmos. and Terr. Phys. 41 (1979) 5-9

Matsushita S. :
Studies in Sudden Commencements in Geomagnetic Storms using IGY Data from United States Stations.
J. Geophys. Res. 65 (1960) 1423-

Matsushita S. :
On Sudden Commencements of Magnetic Storms at High Latitudes.
J. Geophys. Res. 62 (1957) 162-166

Matsushita S. :
On Geomagnetic Sudden Commencements, Sudden Impulses and Storm Durations.
J. Geophys. Res. 67 (1962) 3753-

Matsushita S. and Campbell W.H. (Editors) :
Physics of Geomagnetic Phenomena. Volume I and II
Academic Press, New York and London (1967)

McNamara L.F. :
Model Starting Heights for N(h) Analyses of Ionograms.
J. Atmos. and Terr. Phys. 40 (1979) 543-547

Mirkotan S.G. and Kushnerevskii Yu.V. :
Nonuniform Structure and Motion in the Ionosphere (in Russian).
(Nauka, Moscow 1964)

Namazov S.A., Novikov V.D. and Khmel'nitskii I.A. :
Doppler Shift of Decameter Radio Waves Propagating in the Ionosphere (Review), in Russian.
English Translation in Radio Phys. and Quantum Electron. (1976)

Nelson R.A. :
Response of the Ionosphere to the Passage of Neutral Atmospheric Waves.
J. Atmos. and Terr. Phys. 30 (1968) 825-836

Paul A.K. :
Use of Virtual Height Slopes for Determination of Electron-Density Profiles.
Radio Sci. 2 (1967) 1195-1204

Rishberth H. and Garriott O.K. :
Relationship between Simultaneous Geomagnetic and Ionospheric Oscillations.
Radio Sci. 68D (1964) 339-

Taub H. and Schilling D.L. :
Principles of Communication Systems.
(Mc Graw Hill, 1971)

Titheridge J.E. :
The Relation between Group and Phase Paths in a Non-homogeneous Ionosphere.
J. Atmos. and Terr. Phys. 27 (1965) 1115-1116

Toman K. :
On Waveloke Perturbations in the F Region.
Radio Sci. 11 (1976) 107-119

Toman K. :
Estimating Ionospheric Reflection Height from Doppler Measurements.
IEEE Trans. Antennas and Propagation AP-25 (1977) 273-276

Walton E.K. and Bailey A.D. :
Observation of Seasonal Effects in Travelling Ionospheric Disturbances by the Directional Deviational Technique.
Radio Sci. 11 (1976) 175-178

Watts J.M. and Davies K. :
Rapid Frequency Analysis of Fading Radio Signals.
J. Geophys. Res. 65 (1960) 2295-

Weekes K. :
On the Interpretation of the Doppler Effect from Senders in an Artificial Satellite.
J. Atmos. and Terr. Phys. 12 (1958) 335-338

Yuen P.C., Weaver P.F., Suzuki R.K. and Furumoto A.S. :
Continuous, Traveling Coupling between Seismic Waves and the Ionosphere Evident in May 1968. Japan Earthquake Data.
J. Geophys. Res. 74 (1969) 2256-2264

APPENDIX 1

Times of 1979 SANAE Doppler Recordings

A number of recordings were made during 1979 by Ian Dore, the Ionospheric Physicist at SANAE during this period. Data analysis is not possible as the data will only be available in South Africa in March 1980. It has however been possible to get some idea of the type of data recorded and the conditions prevailing at the time of recording. Table A1 contains a summary of dates and times of recording with solar events indicated if these data were available.

Table A1

Summary of 1979 SANAE Doppler Data

Date	Day No.	Time of recording	Comments
13/6/79	164	13:10 - 13:55 UT	
14/6/79	165	13:10 - 13:55 UT	H_α flare at 13:25 and 13:32 UT
15/6/79	166	13:10 - 13:55 UT	H_α flare at 13:22 UT
16/6/79	167	13:10 - 13:55 UT	H_α flare at 13:40 UT
17/6/79	168	13:10 - 13:55 UT	

Date	Day No.	Time of recording	Comments
9/7/79	190	13:10 - 13:55 UT	H_α flare at 13:47 UT
10/7/79	191	13:10 - 13:55 UT	H_α flare at 13:10 UT
11/7/79	192	13:10 - 13:55 UT	No record
12/7/79	193	13:10 - 13:55 UT	
13/7/79	194	13:10 - 13:55 UT	H_α flare at 13:27 UT
14/7/79	195	13:10 - 13:55 UT	H_α flare at 13:49 UT
15/7/79	196	13:10 - 13:55 UT	
16/7/79	197	13:10 - 13:55 UT	H_α flare at 13:50 UT
5/8/79	217	13:10 - 13:55 UT	
6/8/79	218	13:10 - 13:55 UT	
7/8/79	219	13:10 - 13:55 UT	
8/8/79	220	13:10 - 13:55 UT	
9/8/79	221	13:10 - 13:55 UT	
3/9/79	246	11:10 - 11:55 UT	
4/9/79	247	11:10 - 11:55 UT	
5/9/79	248	11:10 - 11:55 UT	
6/9/79	249	11:10 - 11:55 UT	
7/9/79	250	11:10 - 11:55 UT	

APPENDIX 2

Results from Calculus of Variations

Let the phase path be defined by

$$P = \int_{u_1(t)}^{u_2(t)} F \, du \qquad \text{A2.1}$$

where us is a parameter varying along the curve and is monotonically increasing. The form of F depends on the coordinate system being used. The path can be defined by the parametric equations

$$x_i = x_i(u) \qquad i = 1,2,3 \qquad \text{A2.2}$$

Let $\underline{x}_i(u)$ be the parametric form of another path through $u_1(t)$ and $u_2(t)$ that deviates slightly from the above path. This can be expressed as

$$\underline{x}_i(u) = x_i(u) + \varepsilon \, \eta_i(u) \qquad \text{A2.3}$$

where ε is small and $\eta(u)$ is a differentiable function that vanishes at the endpoints $u_1(t)$ and $u_2(t)$. For the sake of simplicity we define

$$I(\varepsilon) = \int_{u_1(t)}^{u_2(t)} F \, (\underline{x}_i, \dot{\underline{x}}_i, t) \, du \qquad \text{A2.4}$$

and thus

$$I(o) = \int_{u_1(t)}^{u_2(t)} F \, (x_i, \dot{x}_i, t) \, du \; . \qquad \text{A2.5}$$

By Taylor's Theorem

$$I(\varepsilon) = I(o) + \varepsilon \left(\frac{\partial I}{\partial \varepsilon} \right)_{\varepsilon=o} + \ldots\ldots \quad . \qquad A2.6$$

If I(o) has a stationary value, then the condition for an extremum is

$$\left(\frac{\partial I}{\partial \varepsilon} \right)_{\varepsilon=o} = 0 \qquad A2.7$$

which from equation A4 is

$$\left(\frac{\partial I}{\partial \varepsilon} \right)_{\varepsilon=o} = \left(\frac{\partial}{\partial \varepsilon} \left\{ \int_{u_1(t)}^{u_2(t)} F\ (\underline{x}_i, \underline{x}_i, t)\ du \right\} \right)_{\varepsilon=o}$$

$$= \int_{u_1(t)}^{u_2(t)} \left(\frac{\partial}{\partial \varepsilon} \left\{ F\ (\underline{x}_i, \underline{x}_i, t) \right\} \right)_{\varepsilon=0} du \qquad A2.8$$

But from the chain rule

$$\left(\frac{\partial F}{\partial \varepsilon} \right)_{\varepsilon=0} = \left(\frac{\partial F}{\partial \underline{x}_i} \frac{\partial \underline{x}_i}{\partial \varepsilon} + \frac{\partial F}{\partial \underline{x}_i} \frac{\partial \underline{x}_i}{\partial \varepsilon} \right)_{\varepsilon=0}$$

$$= \left(\frac{\partial F}{\partial \underline{x}_i} \eta_i + \frac{\partial F}{\partial \underline{x}_i} \eta_i \right)_{\varepsilon=0} \qquad \text{(Using A2.3)}$$

$$= \frac{\partial F}{\partial x_i} \eta_i + \frac{\partial F}{\partial x_i} \eta_i \quad . \qquad A2.9$$

Equation A8 thus becomes

$$\left(\frac{\partial I}{\partial \varepsilon}\right)_{\varepsilon=0} = \int_{u_1(t)}^{u_2(t)} \left\{ \frac{\partial F}{\partial x_i} \eta_i + \frac{\partial F}{\partial \dot{x}_i} \dot{\eta}_i \right\} du ,$$

which must be equated to zero for an extremum (from A7) yielding the required result, namely

$$\int_{u_1(t)}^{u_2(t)} \left\{ \frac{\partial F}{\partial x_i} \eta_i + \frac{\partial F}{\partial \dot{x}_i} \dot{\eta}_i \right\} du = 0 .$$

APPENDIX 3

Instrumentation tests of the Chirpsounder

A number of tests were carried out on the chirpsounder in order to determine if any of the lines appearing on the Doppler records were of instrumental origin.

A signal generator was used to inject known signals into the spectrum analyser and the output was monitored. The output was always the same as could be predicted from theoretical considerations. It was indicated in Chapter 5 (section 1) how it was possible to determine the build up time of the signal in the spectrum analyser. In two cases, this was found to be 8.5 and 6.0 seconds so that a frequency appearing in the input spectrum appears in the output spectrum after this time.

The Frequency modulation (warble) used to vary the "blind range" of the ionosonde was disabled while recordings were being made and it was found that the signal was unchanged. It is thus concluded that this system does not introduce frequencies into the signal received from the ionosphere.

Similar tests were carried out with the transmitter off, to determine if any "other station interference" could be received and recorded. No signals were recorded during this time, other than the strong signal at 0 Hz known to be caused by RF leakage from transmitter to receiver.

It was concluded that the chirpsounder was not responsible for introducing the lines in the Doppler record and that this structure is present when the signal is received.